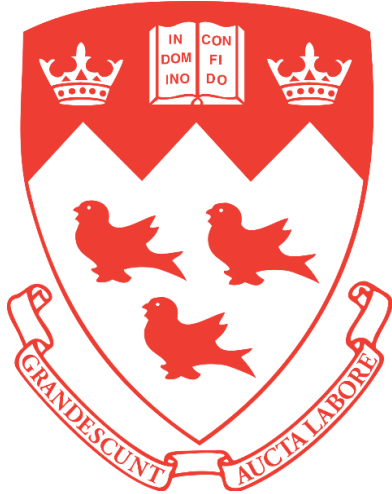


The Analysis of Long-Term Physiological Signals, Brain-Heart Interactions, and periodicities in Patients with Epilepsy



Isaac Reynaud Testa Hassan

Department of Biological and Biomedical Engineering

McGill University, Montreal

August 2022

A thesis submitted to McGill University in partial fulfillment of the requirements
of the degree of Master of Engineering

Acknowledgements

I would like to express my gratitude to my supervisor Georgios D. Mitsis for all his guidance, support, and mentorship throughout the course of this degree. He has provided an excellent example of how scientific research should be conducted and provided me with valuable skills that no doubt will be beneficial in my professional and personal life.

To all my colleagues in the Biosignals and Systems Analysis laboratory, Mohammad Torabi, Xuateng Yuan, Mary Miedema, Emad Askarinejad, Nikos Dimitriou, and Rémi Dagenais, for providing a welcoming environment and providing some much-needed advice, even in the most unforeseen of circumstances, such as the COVID-19 pandemic.

To my parents, Nicole Hassan, and Joseph Testa for their unending and unconditional support throughout my entire studies and for everything that came before. As well as, to my siblings, Michelle, and Alberto Testa who have continue to encourage me at every step of the way.

Lastly, to all the friends who have made Montreal the past few years feel like home.

Contribution of Authors

Dr. Georgios D. Mitsis provided constant feedback and suggestions through the entire research project, access to the datasets and codes for preprocessing both the ECG and EEG datasets.

A previous member of the Biosignals and Systems analysis laboratory, Kyriaki Kostoglou, provided the code for the time varying MVAR model that was crucial for both research Part I and Part II.

Dr. Avgis Hadjipapas greatly contributed to the data analysis methodology, specifically in research Part II for suggestions on the methods for detecting periodicities more consistently among subjects.

Contribution to Original Knowledge

Research Part I:

Different oscillatory components were found in the high frequency and low frequency components of the heart rate variability signal. Correlation with seizure onset with these oscillatory signals was also found to be different depending which component of the heart rate variability was being analyzed. For the low frequency component, correlation was found for circadian periodicity but for the high frequency component, correlation was found for the half-circadian periodicity.

Research Part II:

Time varying coherence between brain and heart data revealed how brain-heart interaction have slow oscillations in a comparable manner to those found in EEG and ECG signals. The theta, alpha and gamma frequency bands were found to oscillate with similar periods, the delta and beta bands were seen deviate from those oscillatory patterns for most subjects.

The average periodograms showed how circadian and half-circadian periodicities were present consistently across subjects and across brain frequency bands. Correlation of these oscillatory components to seizure onset were demonstrated to be dependent on the frequency band and in the coherence between the low frequency component of the HRV and the specific bands. The circadian periodicity of the gamma band showed the most correlation with seizure onset

Abstract:

Background: Epilepsy is one of the most common neurological disorders in the world, affecting approximately 1% of the world's population. It can cause brain activity to become abnormal causing seizures. There are various medical risks associated with seizure onset, as well as a decrease in quality of life for patients diagnosed with epilepsy. However, when it comes to studying physiological signals in patients with epilepsy most of data used to study epileptic seizures are in the short-term surrounding the ictal period (the seizure itself). This assumes that the inter-ictal period is stable, which is at odds with the already established, long-term biological rhythms that are present in physiological signals. So, by studying long-term physiological signals in the context of epilepsy, a better sense of how the complex bodily rhythms present affect physiological signals at time of seizure onset.

Objectives: The main objective this project involved the analysis of long-term analysis of physiological signals from subjects with epilepsy, as well as the determination of the periodic components on those signals and their correlation with seizure onset.

Methods: This project was divided in two parts with different datasets used for each one. In Part I, an HRV signal was built from the detected R peaks of the ECG signals. The HRV was then fed into an MVAR model, and the power spectral density matrices were computed. The HF and LF components of the HRV were isolated and their periodicities were estimated. Circular statistics were then used to calculate the correlation of the periodic signal to seizure onset. In Part II, the mean intracranial EEG signal was computed, the five frequency bands were extracted, and their envelope is computed. Then the HRV and EEG-ENV were fed into the MVAR model, then power

spectral density matrices and coherence were computed. The periodicities were estimated, and finally circular statistics was used to compute the correlation to seizure onset in group level and in a subject specific manner.

Results: For Part I, the main periodic components seen in the HRV, HF and LF signals were at approximately four, twelve and twenty-four hours. Correlation with seizure onset were seen in the HF signal at the twelve-hour periodicity and in the LF signal at the twenty-four periodicity. For Part II, the time-varying coherence of the theta, alpha, and gamma bands with the HRV-LF were more coupled, however the delta and beta bands were the most distinct ones. The periodicities detected in the EEG envelopes were distributed in a more spread-out way than the HRV-LF. The time-varying coherence had less periodic components then the EEG-ENV and HRV-LF signals. Correlation with seizure onset had a wide assortment of variation across subjects and frequency bands. At a group level, the strongest correlations detected were for the circadian periodicities of the HRV-LF and the Gamma-ENV.

Abstrait (French)

Contexte : L'épilepsie est l'un des troubles neurologiques les plus courants dans le monde. Elle touche environ 1 % de la population mondiale. Elle peut provoquer une activité cérébrale anormale à l'origine de crises d'épilepsie. Il existe divers risques médicaux associés à l'apparition de crises, ainsi qu'une diminution de la qualité de vie des patients diagnostiqués épileptiques. Cependant, lorsqu'il s'agit d'étudier les signaux physiologiques chez les patients épileptiques, la plupart des données utilisées pour étudier les crises épileptiques portent sur le court terme entourant la période ictale (la crise elle-même). Cela suppose que la période inter-ictale est stable, ce qui est en contradiction avec les rythmes biologiques à long terme déjà établis qui sont présents dans les signaux physiologiques. Ainsi, l'étude des signaux physiologiques à long terme dans le contexte de l'épilepsie permet de mieux comprendre comment les rythmes corporels complexes présents affectent les signaux physiologiques au moment de l'apparition des crises.

Objectifs : L'objectif principal de ce projet était l'analyse à long terme de signaux physiologiques provenant de sujets épileptiques, ainsi que la détermination des composantes périodiques sur ces signaux et leur corrélation avec le déclenchement des crises.

Méthodes : Ce projet a été divisé en deux parties. Dans la première partie, un signal HRV a été construit à partir des pics R détectés des signaux ECG. Le VRC a ensuite été introduit dans un modèle MVAR, et les matrices de densité spectrale de puissance ont été calculées. Les composantes HF et LF du HRV ont été isolées et leurs périodicités ont été estimées. Des statistiques circulaires ont ensuite été utilisées pour calculer la corrélation entre le signal périodique et le début de la crise. Dans la deuxième partie, le signal iEEG moyen a été calculé, les

cinq bandes de fréquence ont été extraites et leur enveloppe a été calculée. Ensuite, le HRV et l'EEG-ENV ont été introduits dans le modèle MVAR, puis les matrices de densité spectrale de puissance et la cohérence ont été calculées. Les périodicités ont été estimées, et enfin les statistiques circulaires ont été utilisées pour calculer la corrélation avec l'apparition des crises au niveau du groupe et d'une manière spécifique au sujet.

Résultats : Pour la première partie, les principales composantes périodiques observées dans les signaux VRC, HF et LF se situaient à environ quatre, douze et vingt-quatre heures. La corrélation avec le début des crises a été observée dans le signal HF à la périodicité de douze heures et dans le signal LF à la périodicité de vingt-quatre heures. Pour la partie II, la cohérence variable dans le temps des bandes thêta, alpha et gamma avec le VRC-LF était plus couplée, cependant les bandes delta et bêta étaient les plus distinctes. Les périodicités détectées dans les enveloppes de l'EEG étaient distribuées de manière plus étalée que celles du HRV-LF. La cohérence variable dans le temps avait moins de composantes périodiques que les signaux EEG-ENV et HRV-LF. La corrélation avec le début des crises présentait un large éventail de variations selon les sujets et les bandes de fréquence. Au niveau du groupe, les plus fortes corrélations détectées concernaient les périodicités circadiennes du VRC-LF et du Gamma-ENV.

Table of Contents

Acknowledgements.....	ii
Contribution of Authors.....	iii
Contribution to Original Knowledge	iv
Abstract:.....	v
Abstrait (French)	vii
Table of Contents.....	ix
List of Figures	xi
List of Tables	xii
List of Abbreviations	xiii
Chapter 1: Introduction	1
1.1 General Introduction.....	1
1.2 Project Objectives	3
1.3 Datasets	4
Chapter 2: Literature Review	7
2.1 The Autonomic Nervous Systems	7
2.2 ECG and The Heart-Rate Variability Signal.....	8
2.3 ANS and Cardiovascular system in Epilepsy.....	11
2.5 Brain – Heart Interactions.....	13
2.6 Intracranial EEG.....	15
Chapter 3: Research Part I – Long Term properties of HRV in Epilepsy	19
3.1 Preface to Research Part I.....	19
3.2 Methods:.....	19
3.2.1 Pre-process	19
3.2.2 QRS-detection	20
3.2.3 MVAR-Model.....	21
3.2.4 HRV, HF, and LF isolation	22
3.2.5 Periodicity Estimation	23
3.2.6 Hilbert Transform.....	24
3.2.7 Circular Statistics, Rayleigh Tests, and correlation with seizure onset.....	25
3.3 Results.....	26

3.3.1 Signals preprocessing, QRS detection and spectrograms	26
3.3.2 Detection of periodic components	29
3.3.3 Filtered periodic signals and seizure correlations.....	31
Chapter 4: Research Part II – Long Term Brain Heart Interactions in Epilepsy.....	35
4.1 Preface to Research Part II.....	35
4.2 Methods	36
4.2.1 Envelope of iEEG signals	36
4.2.2 Coherence	37
4.2.3 Periodicity Estimation	38
4.2.4 Correlation with seizure onset.....	39
4.3 Results	39
4.3.1 Brain-heart interactions for all the frequency bands	39
4.3.2 Detection of periodic components	42
4.3.3 Seizure onset correlation with periodic signals at the group level.....	47
4.3.4 Seizure onset correlation at the individual level	51
Chapter 5: Discussion.....	53
Research Part I	53
Research Part II	55
Chapter 6: Conclusion and Future Work.....	59
Bibliography:	61
Appendix:	67
Appendix A: Brain-heart interactions for all subjects.....	67
Appendix B: Histograms of detected periodicities for each signal	72
Appendix C: Average Periodograms for each signal	74

List of Figures

Figure 1: Distribution of intracranial EEG electrodes	6
Figure 2: Typical ECG waveform with one RR interval represented.....	9
Figure 3: Increase in the number of publications related to intracranial EEG data	16
Figure 4: A representation of the two types of intracranial EEG electrodes.....	17
Figure 5: Processing pipeline of R peak detection based on Pan-Tompkins detection algorithm	20
Figure 6: Extract of ECG signal from one subject.....	27
Figure 7: Spectrograms of HRV computed from two of the subjects.....	28
Figure 8: Examples of the three-time series derived from the MVAR model for two of the subjects.....	29
Figure 9: Periodograms obtained for subject 03	30
Figure 10: Examples of the filtered periodic signals from subject 03	32
Figure 11: Angular plots for statistically significant correlations	34
Figure 12: Processing scheme research part II	36
Figure 13: Extract of the Envelope computed for Gamma envelope of EEG band of subject 07.....	40
Figure 14: Time series used in Part II.....	41
Figure 15: Time-varying coherence between HRV-LF and each EEG-ENV.....	42
Figure 16: Autocorrelation plots for signals	43
Figure 17: Periodograms for time signals	44
Figure 18: Histograms with distribution of periodicities detected.....	45
Figure 19: Average periodograms	46
Figure 20: Angular plots for three circadian periodicities seizure correlation analysis.....	49
Figure 21: Seizure correlation for HRV-LF for subject 6	51
Figure 22: Seizure correlation for coherence between HRV-LF and Gamma-ENV for subject 10.....	52

List of Tables

Table 1: List of subjects used for part 1.....	5
Table 2: List of subjects used for part 2.....	6
Table 3: Detected periodicities for each subject in Part I.....	31
Table 4: p-values from Rayleigh test	32
Table 5: R value obtained from angular plots	33
Table 6: Correlation of seizure onset with periodic signals.....	49
Table 7: Bootstrap results for circadian periodicity	50
Table 8: Bootstrap results for half-circadian periodicity	50

List of Abbreviations

AED – Antiepileptic drug

ANS – Autonomic Nervous System

AR – Autoregressive

CNS – Central Nervous System

dB – Decibels

ECG – Electrocardiogram

ECoG - Electrocorticography

EEG – Electroencephalogram

ENV – envelope

FFT – Fast Fourier Transform

GC – Granger Causality

h - Hours

HF – High Frequency

HR – Heart Rate

HRV – Heart Rate Variability

Hz – Hertz

iEEG - Intracranial electroencephalography

LF – Low Frequency

ms - Milliseconds

mV – millivolts

PLI – Phase Lag Index

PLV – Phase Locking Value

PSD – Power Spectral Density

SNR – Signal to Noise ratio

SUDEP – Sudden Unexpected Death in Epilepsy

TDS – Time Delay Stability

TE – Transfer entropy

TFD – Time frequency distribution

TV-MVAR – Time-varying multivariate autoregressive model

VLF – Very Low Frequency

Chapter 1: Introduction

1.1 General Introduction

Epilepsy is one of the most common neurological disorders in the world, affecting approximately 1% of the world's population [1]. Having a bimodal onset which occurs most commonly in early childhood and older adults, it can affect people of all ages with a wide range of severity and impacts [2]. It can cause brain activity to become abnormal causing seizures. These seizures are caused by disturbance in the electrical activity of the brain due to a hypersynchronous discharge of neurons. Three distinct categories are used to describe them: generalized seizures, focal seizures, or epileptic spasms. Generalized seizures originate simultaneously from both hemispheres of the brain, focal seizures are ones where EEG or clinical evidence can be seen that the seizure originated from a localized area within a single hemisphere, and epileptic spasms refers to seizures that invoke sudden extensions or flexion of extremities [1, 3].

There are various medical risks associated with seizure onset, as well as a decrease in quality of life for patients diagnosed with epilepsy [4]. A higher prevalence of depression, cognitive difficulties, mood disorders, and other psychiatric disorders are seen compared to the general population [5]. Bone health problems such as low bone density or osteoporosis are commonly observed, this is due to the long-term use of Antiepileptic drugs (AEDs). AEDs have an effect on vitamin D resulting in calcium deficiency [6]. It was seen that the relative risk of fractures

was generally higher as well; with a sevenfold risk of seizure-related femur fractures in institutionalized patients, and a twofold risk of fractures for non-institutionalized patients [7]. An increasing amount of comorbidities have been associated with epilepsy and seizure onset, many of which have bidirectional relations, causing a great deal of distress and tribulations on the patients, this has led to a great deal of interest in how to improve the quality of life of these patients [8].

Due to all the complications that arise because of epilepsy, there has been considerable interest in developing seizure detection and prediction algorithms. These algorithms could be used to avoid injuries, providing therapies in times of seizure susceptibility and abort seizure through targeted therapy [9]. One of the difficulties for the construction of general usage algorithms is that most of the physiological signals used to study epileptic seizures are in the short-term surrounding the ictal period (the seizure itself) [10]. This assumes that the inter-ictal period is relatively stable, which is at odds with the already established, long-term biological rhythms that are present in physiological signals. The bodily rhythms present show complex dynamics and large oscillations that can cause false seizure predictions, so considering the circadian periodicities when studying physiological signals can lead to a decrease of false positives [11, 12]. It was found seizure onset correlated strongly to periodic components of functional brain networks obtained from EEG in long term data [10]; thus further demonstrating the need of studying long term physiological signals in the context of epilepsy.

1.2 Project Objectives

The broad objectives of this project involved the analysis of long-term analysis of physiological signals from subjects with epilepsy. The physiological signals studied were the electrocardiogram (ECG) signals of the heart and the intracranial electroencephalography (iEEG) signals of the brain. The idea behind looking at these signals was so that the long-term biological rhythms are considered when studying physiological signals from subjects with epilepsy, so as to be able to understand how these rhythms affect seizure onset. The project was divided into two parts, each with their own general and specific objectives:

Part I: The analysis of long-term heart rate variability (HRV) and the correlation of its periodicities to epileptic seizure onset.

Part II: The analysis of long-term brain-heart interactions between frequency bands from the brain signals and the heart rate variability, and the correlation to epileptic seizure onset.

For **Part I**, the specific objectives involved: Quantifying the long-term periodic patterns in the HRV signal and in the high frequency (HF) and low frequency (LF) power; then, investigating whether seizure onset is correlated with these periodic patterns.

For **Part II**, the specific objectives involved: First, Quantifying the interactions between iEEG and ECG, more specifically, the coherence between the frequency bands from the brain and the LF components of the HRV; then, quantifying the long-term periodic patterns that are present in all those time series, and finally Investigating whether seizure onset is correlated with these periodic patterns in both a group level basis, and an individual level basis.

1.3 Datasets

Two datasets were used for this project, both containing long-term physiological recordings of the brain and of the heart.

The first dataset was recorded at the Neurology Ward of the Cyprus Institute of Neurology and Genetics and contains the EEG and ECG signals. Seizures and sleep intervals were marked by specialized neurophysiologists. Out of the ten subjects, one of them did not have a seizure during the recording, two of them had recording session of less than 24 hours, and two of them had the data corrupted and thus have not been able to be used. Out of the ten subjects, six of them were recorded using the XLtek EEG recording system at 200 Hz, and the other four were recorded using the Nicolet system at 500 Hz. **Table 1** shows a summary of the subjects considered in this dataset with their respective length of recording and number of seizures. From this dataset only the ECG signals were considered. This dataset was used for Part I.

SUBJECT	RECORDING LENGTH (HOURS)	NUMBER OF SEIZURES
1	69	4
2	21	1
3	67	2
4	22	2
5	66	2
6	45	1
7	27	6

8	24	0
---	----	---

Table 1: List of subjects used for part 1

The second dataset was recorded at the clinical neurophysiology department at the Maastricht university hospital from patients who underwent examination for candidacy of epileptic surgery, and it contains long term recordings of iEEG and ECG signals. Out of the full dataset, 12 subjects were considered. One of the subjects did not have a seizure in the length being considered. The recordings were sampled at 2048 Hz. **Table 2** shows a summary of the subjects considered with their respective length of recording and number of seizures. **Figure 1** shows the placement of the intracranial EEG electrodes for one of the subjects. This dataset was used for Part II.

SUBJECT	RECORDING LENGTH (HOURS)	NUMBER OF SEIZURES
1	229	36
2	165	38
3	102	8
4	170	16
5	145	37
6	189	22
7	173	21
8	171	78
9	142	80
10	211	18

11	91	22
12	90	0

Table 2: List of subjects used for part 2

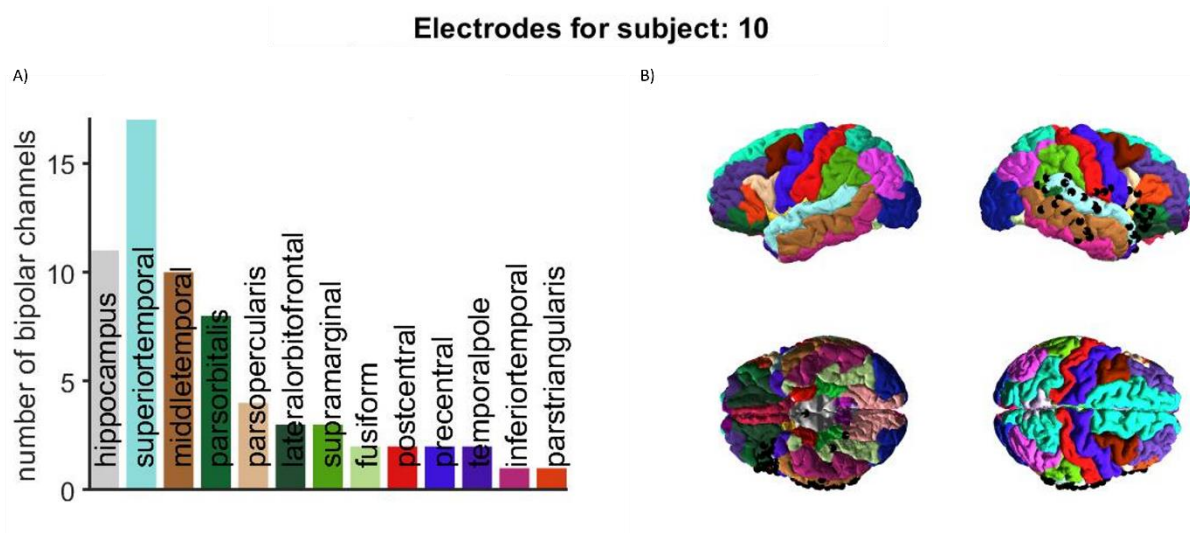


Figure 1: Distribution of intracranial EEG electrodes

- A) Shows the number of electrodes in each brain region close to zone of epileptic lesion.
 B) Location of electrodes in the brain

Chapter 2: Literature Review

2.1 The Autonomic Nervous Systems

Epileptic seizures will alter the function of the Autonomic Nervous system (ANS) [13]. The ANS, plays a role in maintaining the homeostasis in the body, functions without any conscious, voluntary control. It engages in the regulation of blood pressure, gastrointestinal responses to food, contraction of the urinary bladder, focusing of the eyes, and thermoregulation. It can be divided into two functionally and anatomically different divisions: the sympathetic system and the parasympathetic system [14]. The sympathetic response is activated during stressful situations regulates the “fight or flight” response, its output to the heart is controlled by neurons from the rostral ventrolateral medulla and can cause increase in atrio-ventricular conduction and ventricular excitability, resulting in increased heart rate. The parasympathetic response regulates the “rest and digest” response, its output to the heart is controlled by the vagus nerve, increases vagal efferent activity, ventricular excitability, and atrioventricular conduction, resulting in a decrease of heart rate [15, 16]. In order to study the ANS, the heart rate variability (HRV) signal obtained from the heart, and more specifically its high frequency (HF) and low frequency (LF) components of the heart rate variability are used as a proxy measurement [17].

2.2 ECG and The Heart-Rate Variability Signal

The HRV is obtained from the ECG signal, which represents the electrical activity of the heart. A typical ECG waveform consists primarily of a P wave, a QRS complex, and a T wave; where the P wave happens during atrial depolarization, the QRS complex represents depolarization of the ventricles, and the T wave represents repolarization of the ventricles [18]. From this ECG signal, an HRV time-series can be obtained by obtaining the distance between the R peaks of adjacent QRS complexes. **Figure 2** shows what a typical ECG waveform looks like with the interval between two R peaks signaled.

Something to consider when working with the ECG signal is the sort of noise it could be subject to. The most common type of noises identified in ECG are, Powerline interference, Baseline Wander, Muscle Artifacts and Electrode movement noise [19]. Power line interferences are sources of noise that occur due to power lines and cables present in the ECG data collection; this can be caused by magnetic induction in the cables, loops in cables, electromagnetic waves in nearby equipment, etc. Baseline wander is a low frequency component noise that occurs due to breathing, changes in respiration. Muscle artifacts occur due to muscle activity during the ECG recordings. Electrode movement noises are cause by the movement of electrodes which in turn causes the skin to stretch, and causes changed in impedance between skin and electrode. These are the most difficult to remove since their spectrum can completely cover the ECG signal and has similar morphology to the P, QRS and T waves [20, 21].

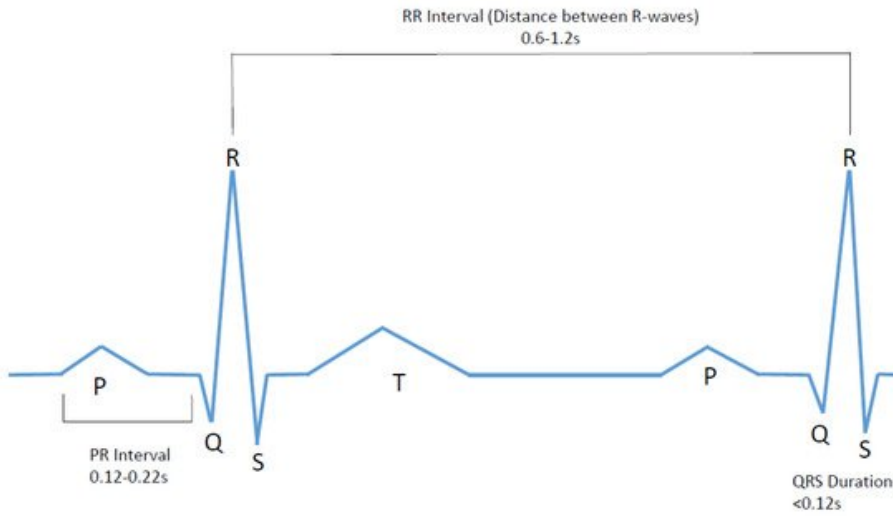


Figure 2: Typical ECG waveform with one RR interval represented [18]

Once the HRV signal is obtained, which correspond to a time series of R peak events, the signal can be decomposed to three principal components: a Very Low Frequency (VLF), Low Frequency (LF), and High Frequency (HF). **VLF** is characterized by a frequency range of 0 – 0.04 Hz; **LF** by a range between 0.04 – 0.15 Hz; and **HF** by a range of 0.15 – 0.4 Hz [22]. LF has been related to both sympathetic and parasympathetic activities, the HF has been related exclusively to the parasympathetic system activation [15].

One aspect that has to be considered when working with HRV signal is that it is a stochastic process whose points are non – equidistant, meaning that two neighboring points are not continuous functionally dependent from one another, which can create issues when performing spectral analysis of HRV to be used as the proxy measurement for the ANS.

In order to study the changes in power spectra over time, the spectrogram has to be computed. Generally, the most common way of computing a spectrogram is through the usage of sliding window of fast Fourier transform (FFT). However; this method can be problematic when using the HRV signal due to the fact that points have to be equidistant for the sliding FFT, and interpolation could introduce biases in shorter time segments [23]. There are a few methods that have been proposed for adapting the FFT for its usage in HRV analysis. The most common techniques are: One way is by interpolating between the points to obtain equidistant values; however, this will cause the problem of actually replacing the measured values, this is especially important when considering that beat to beat are point event, with no values in between. Another approach is to obtain the mean of the HRV values and usage to build equidistant steps, the purpose of this is so that the measured values do not change. However, by doing this we are distorting the rhythm, creating a series of equidistant points that would have a constant value [22, 23].

Some of the other methods that are used for HRV spectral analysis are time-frequency distribution (TFD) methods such as the Wigner Ville Distribution, and autoregressive models [23, 24]. With autoregressive models being the most suitable ones as they provide better frequency resolution [25].

TFDs are an approach used for non-stationary process that describes the frequency content of the signal as function of time. The choice of which TFD is used has to be done for each signal depending on its characteristics, the most common one being the quadratic TFD, whose general form can be seen in **Equation 1** [26].

$$\rho_z(v, f) = \iint_{-\infty}^{\infty} g(v-u, \tau) z \left(u + \frac{\tau}{2} \right) z * (u - \tau 2) e^{-j2\pi f t} du d\tau \quad \text{Eq. 1}$$

The Wigner Ville distribution is the most common TFD used for HRV spectral analysis, which correspond to the case in the quadratic TFD where $g(v, \tau)$ is equal to one.

Time varying autoregressive models are another commonly used to represent nonstationary signals and perform spectral analysis in the HRV signal. They work by estimating the value of the signal at time point t value by using previous values and a constant a which is usually estimated by method of least squares and an error function. At each time point t , the Z transform can be used to compute the instantaneous PSD [23].

2.3 ANS and Cardiovascular system in Epilepsy

The output of the autonomic nervous system into the heart gets regulated by brain structures as the prefrontal cortex and insular cortex, the amygdala, one of the lateral regions of the hypothalamus, several regions of the medulla, and a few other structures such as: BNST (ben nucleus of stria terminalis), PVN (paraventricular nucleus), DMH (dorsomedial hypothalamic nucleus), and PAG (periaqueductal grey matter of the midbrain), and a region of the lateral pons. The medulla integrates all this information from the various reflex centers, and there a distinction can be made between parasympathetic activity and the sympathetic activity [16].

Epileptic seizures can cause abnormalities in the ANS leading to a dysfunction in the operation of the cardiovascular system and in the heart. Patients with epilepsy tend to have lower HRV values than the healthy population [27, 28]. It has also been reported that there is an increase of heart rate seen in a high proportion of seizures, one study showing that the average HR of patients (78 beats/min) went up for 93% of patients (73% of seizures) by 10 beats/min or more; and for 80% of patients (55% of seizures) by 20 beats/min or more [29]. During epileptic seizure, ECG abnormalities can be frequently seen, in one study there were reported in 26% of seizures (which corresponded in 44% of the subjects); with those abnormalities commonly characterized by a steep acceleration phase and wide fluctuations during and immediately after the seizure onset [29]. As for changes that are seen in the frequency spectra, epilepsy patients showed to have lower values of HF-HRV, with a trend of higher values of LF for subjects receiving treatment [28]. All of these findings indicate that there is a direct effect in the ANS that stems from epilepsy and epileptic seizure onset, creating a sympathovagal imbalance.

One other reason to study the effects of the cardiovascular system in patients with epilepsy is because of Sudden Unexpected Death in Epilepsy (SUDEP). SUDEP refers to the unexpected death of a patient with epilepsy where post-mortem examination does not reveal a structural or toxicological cause of death, and that it was not caused by seizure onset [30]. It is estimated that approximately 15% of epilepsy related deaths could be attributed to SUDEP [31]. The mechanism of how SUDEP occurs is currently unknown; however, the various hypothesis of how it occurs point to the fact that it seems to be related to autonomic dysfunction or sympathovagal imbalance and abnormalities in cardiac mechanisms [13, 28]. It has even been proposed that HRV could be a potential biomarker of SUDEP risk [32]. By further studying and

understanding the relation of epilepsy and epileptic seizures onset with the ANS and its cardiovascular systems, a better understanding of why SUDEP occurs could be achieved, as well as eventually perhaps find practical clinical markers for it.

2.5 Brain – Heart Interactions

The study of brain-heart interactions is referred to as the study of the interaction between the cortical activity in the central nervous system (CNS) and the ANS [33]. This has become an emerging field of study which aims to take advantage of the advances in neuroimaging, signal processing and network science to obtain a more complete understanding of a complex physiological system. Moreover, there has been evidence for clinical implications of dysfunctional brain heart interactions [34]. For example, in older patients suffering from nonrheumatic atrial fibrillation, the most frequent arrhythmia in older patients, and without previous incidence of a stroke, a lower Mini-Mental State Examination score was seen than in a reference group, indicating that atrial fibrillation may cause a cognitive disorder [35].

In order to study these brain-heart interactions numerous approaches are used, the most common ones being Granger Causality (GC), information transfer approaches such as transfer entropy (TE) and time-delay stability (TDS), phase synchronization approaches such as phase-locking values (PLV) or phase lags indexes (PLI) and time variant and frequency selective approaches such as time-frequency analysis and coherence measurements [33, 36-38]. The

choice of which one of these approaches to be used has to be determined based on the goals of the specific study in mind.

GC is a statistically tool to determine if one signal can be used to predict the value of another signal. If a signal X_1 “Granger-cause” a signal X_2 , then the past values of X_1 can be used to predict future values of X_2 [39]. GC is also widely used in studies in functional neuroimaging, where the aim is to understand the relationship between specific brain areas and mental functions [40].

TE is a non-parametric measure of how information is transferred between two signals. It is particularly useful when evaluating nonlinear couplings without the need for a priori information [41, 42].

TDS is a network-based approach used to study the dynamics of multiple interconnected systems as they transition from one physiological state to another; in other words, it determines which changes in the output of a given system are consistently followed by corresponding modulations in the signal output of another system [36].

PLV and PLI are non-parametric estimates of phase synchronization that do not depend on the amplitude of the signals and aim to elucidate the consistency of phase difference between two signals [43]. PLV evaluates the instantaneous phase difference between the two signals, this assumes that in sections of the signals that are coupled, the oscillation properties of their phases will be connected and thus the phases will evolve together. If this is the case then the difference between the phases will be constant and the signals are said to be phase-locked [44]. The concern that arises when it comes to PLV is the fact that in the present of common source, the phase

synchrony detected would be biased. In order to reduce that bias, the concept of PLI is can be introduced. PLI disregards the phase locking that is centered around zero mod π and defines an asymmetry index for all the phase differences. When phases are distributed around a difference of zero, no phase coupling exists, and a deviation from this flat distribution will indicate phase synchronization [45].

Time variant and frequency selective approaches can be used to analyze acute changes in both the EEG and ECG-HRV signal as representing these signals in a time-frequency spectra allows to analyze how these signals behave across time in a specific frequency range of interest, hence these same techniques can be used to study the interactions between those signals [46, 47]. The most common method used in this approach is the coherency measurement, which characterizes the linear relationship between two variables in the frequency domain. It can be interpreted as the proportion of the power of one time series that can be explained by its linear regression on the other series at a given frequency [38].

2.6 Intracranial EEG

To study brain-heart interactions, high quality brain and heart signals need to be used. A neuroimaging modality that is becoming more common both in clinical applications and research is intracranial EEG (iEEG). A downside being that adoption of is highly dependent on highly trained professionals **Figure 3** shows how its usage has been increasing throughout the years [48]. For clinical applications in the context of epilepsy, it is used primarily for the evaluation of the surgical

candidacy, more specifically for the localization of the seizure onset zone. For many patients, non-invasive modalities can localize the seizure onset zone; however, a study showed that 30–40% of patients considered for would likely benefit from intracranial evaluation [49].

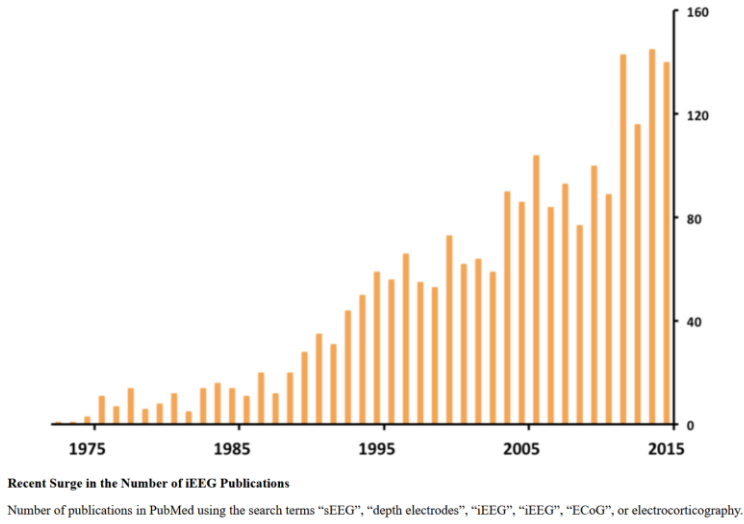


Figure 3: Increase in the number of publications related to intracranial EEG data [48]

Although there are various methods and types of electrodes, the two main ones are subdural strips (or grids) and depth electrodes, which is called Electrocorticography (ECoG) [50]. While grids and strips of subdural electrodes provide a large coverage over the bare surface of the cerebral cortex, they are often implanted in one hemisphere and do not reach deeper brain structures. The other commonly implanted are the depth electrodes which can enable bilateral monitoring of superficial and deep cortical structures. A combination of the several types of electrodes is used quite often, especially in monitoring for candidacy of epilepsy surgery, which allows for a larger coverage of the brain area [48, 51].

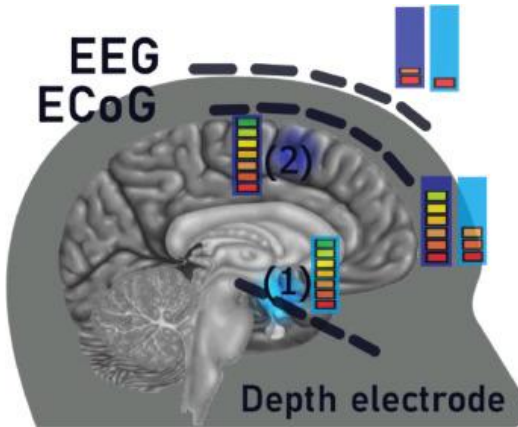


Figure 4: A representation of the two types of intracranial EEG electrodes. The color bar shows the strength of the signal being recorded. The difference in signal strength between scalp EEG and both modalities of intracranial EEG can be noted [51].

iEEG has various advantages over scalp EEG such as: higher SNR, sparse sampling and broad spatial coverage, and higher temporal resolution. iEEG has a SNR that can be as high as one hundred times higher than in scalp EEG. This is in part because of $\sim 10x$ higher amplitude of iEEG signal compared to scalp EEG, and significantly reduced problem of electro-magnetic noise from the recording room, physiological noise from cardiac signal or muscle contractions, or skin potentials (e.g., skin cells on the scalp or ionic potential of sweat glands) with intracranial recordings [48]. Because iEEG electrodes are dictated by clinical need of implantation in each patient, it allows for a more personalized recording set up. As well as providing the opportunity for excellent global coverage across the whole brain. Implantations typically have around 150 to 200 different recording sites allowing to cover a wide range of regions. The temporal resolution allows for a sampling rate between 1000 Hz and 3000 Hz. Even if conventional scalp EEG and MEG can record at a similarly high sampling rate, the iEEG signal being highly localized it provides a source of signal that is more spatially defined, allowing the observation of fast

dynamics between precisely localizable populations of neurons across distinct brain regions [48, 50].

Chapter 3: Research Part I – Long Term properties of HRV in Epilepsy

3.1 Preface to Research Part I

In order to complete the general and specific objectives for Part I, first the ECG signal was processed to obtain the three relevant time-series, the HRV, HF, and LF. Periodicities were detected in those three signals, and then correlation to seizure onset was computed.

3.2 Methods:

3.2.1 Pre-process

The ECG dataset was extracted from the total dataset. For the patients whose data was recorded using the Nicolet system, the data was down sampled to 200 Hz, for the patients whose data was recorded using the XLTek system, the data was not resampled.

The data was bandpass filtered between 0.5 Hz and 60 Hz using a second order Butterworth Filter with a passband rippled of 5 dB and a stopband attenuation of 20 dB. The filtered data was then examined, and a threshold was applied based on the motion artifacts that were present in the data, which in some cases were significant, due to the fact that the data was recorded for extended periods of time.

3.2.2 QRS-detection

A QRS detection algorithm based on the Pan-Tompkins methods was utilized on the filtered ECG signal in order to obtain the HRV signal [52]. This algorithm starts by applying a set of filters; first a low pass filter, then a high pass filter, differentiation is then performed to obtain information about the QRS slope. The signal is then squared to intensify the slope and help distinguish it from the T wave. A moving integration window is used to obtain the width of the QRS complex. The adaptive threshold that the algorithm uses to decide on the QRS complex are based on the amount of noise detected, which is obtained by the filtering process. Further processing was done to shift ectopic beats, and smooth out dubious areas of the tachogram. From the tachogram obtained, the HRV was obtained by creating a time series of the interval between each R peak. The data was then smoothed out, then subtracted by its mean and then divided by its standard deviation.

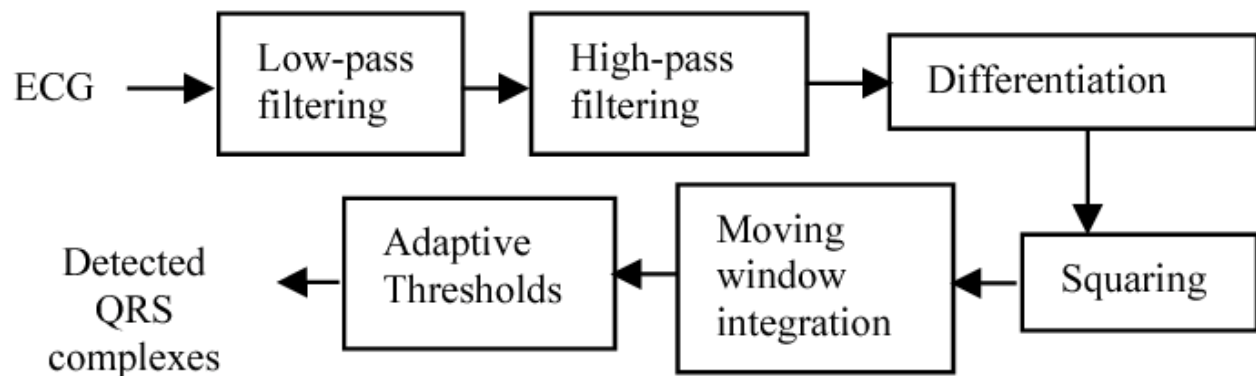


Figure 5: Processing pipeline of R peak detection based on Pan-Tompkins detection algorithm [53]

3.2.3 MVAR-Model

In order to obtain a time-frequency representation of the HRV, an Autoregressive model (AR) was used to obtain a time series with points that are equidistant. The autoregressive model used was one proposed by a previous member of the Biosignals and Systems analysis laboratory [54]. The time-varying model, estimates the next point in the time series, based on the last points by using a Kalman Filter. The difference between a conventional AR based model and the one being used is that it estimates the noise covariance matrix at each step recursively. This is done so that parameters that exhibit large fluctuations are assigned larger covariance matrices than parameters with slow and small fluctuations as well as to address the fact that time-varying parameters may be characterized by a mixture of slow, fast, and abrupt variations. The general form of the MVAR model is represented by **Equation 2**.

$$y(n) = \sum_{k=1}^P A_k(n) y(n - k) + \varepsilon(n) = A(n)\Phi(n) + \varepsilon(n)$$

Eq. 2

For this application, y , is the obtained time series corresponding to the HRV. A_k corresponds to a time-varying autoregressive matrix for each model order k . $\varepsilon(n)$ was assumed to be a zero-mean white noise vector. The maximum model order used was ten.

The application of this model was used to accomplish various things: First, create a signal that is equidistant and sampled at regular intervals throughout its entirety. Then, to make up for

any potential gaps that were present due to the highly corruptible motion artifacts present in the original ECG signals. Lastly, to obtain a time-varying spectral density matrix of the HRV signal, which is obtained through **Equation 3**.

$$S(f, t) = He(f, t) \sum He^{He}(f, t) \quad \text{Eq. 3}$$

$$He(f, t) = [I - A(f, t)]^{-1} \quad \text{Eq. 4}$$

$$A(f, t) = \sum_{k=1}^p A_k(t) e^{-i2\pi f k T} \quad \text{Eq. 5}$$

Where $He(f, t)$, the Hermitian transpose, is the time-varying transfer matrix in the frequency domain as time point t and $A(f, t)$ is the time-varying coefficient matrix.

3.2.4 HRV, HF, and LF isolation

After obtaining the spectrogram for the HRV from the MVAR model, the high-frequency component (0.15-0.40 Hz) and low-frequency components (0.04-0.15 Hz) were isolated. Then, a time-series based on the average of a band surrounding the peak of the frequency component

was obtained. Three time-series are obtained, one for the HRV, one for the HF component and one for the LF component.

3.2.5 Periodicity Estimation

In order to assess the periodicities of the three time-series, the periodogram was computed for each one of them. The periodograms were computed by first computing their autocovariance (s_k), and then performing the FFT on those autocovariances obtained. **Equation 6** was used to compute the autocovariance of a signal, and **Equation 7**, which denotes Fourier transform pairs, was used to obtain the periodograms.

$$s_k = \frac{1}{n} \sum_{i=1}^{n-k} (y_i - \bar{y})(y_{i+k} - \bar{y}) \quad \text{Eq. 6}$$

$$PSD(f) = \sum_{\tau=-\infty}^{\infty} s_k e^{-2i\pi f\tau} \quad \text{Eq. 7}$$

Periodicities were assessed by plotting these periodograms in terms of the inverse of the frequency to obtain the period and assessing where significant peaks were present. To obtain band-limited signals around those detected components the periodicities were isolated by using

a zero-phase filter, which causes no phase distortion or time-delay. For each detected periodicity, ± 1 hours were considered.

3.2.6 Hilbert Transform

Once the periodic signals were obtained for all detected periodicities on each of the time-series, the Hilbert transform was calculated for each of the periodicities. The Hilbert transform can be used as a method for obtaining the magnitude and phase information from a signal. The Hilbert transform is calculated using **Equation 8**.

$$H[x(t)] = \frac{1}{\pi} PV \int_{-\infty}^{\infty} \frac{x(\tau)}{t - \tau} d\tau \quad \text{Eq. 8}$$

Where PV refers to the Cauchy Principal Value, which is a method of assigning a value to an improper integral which otherwise could be undefined [55]. In this scenario, the Hilbert transform was applied to the band limited periodic signal to obtain the instantaneous phase for each of the periodicities.

3.2.7 Circular Statistics, Rayleigh Tests, and correlation with seizure onset

The circular nature of the data considered will cause the usage of commonly used statistical techniques to provide wrong or misleading results. In order to assess whether seizure onset correlate to specific periodic components of any of the three-time series, circular statistics was used. Circular statistics is a useful tool for data in an angular scale, where there is not a designated zero [56].

The instantaneous phases at the moment of seizure onset were wrapped from 0 to 2pi, and a mean resultant vector was calculated, which represented the average direction of the circular data. The length of that mean vector, R, was also obtained, as it can be used as a measurement of the circular spread or can be used for hypothesis testing in directional statistics. The closest R is to one, the more concentrated the data sample around the mean direction is.

The mean resultant vector is computed using **Equation 8**, and the resultant vector length through **Equation 9**, where r_i are the directions transformed to unit vectors in the two-dimensional plane:

$$\bar{r} = \frac{1}{N} \sum_i r_i \quad \text{Eq. 8}$$

$$R = \|\bar{r}\| \quad \text{Eq. 9}$$

In order to do hypothesis testing, Rayleigh test can be used to determine if the data is uniformly distributed among a circle. If the Null Hypothesis is rejected (obtained p value less than 0.05) it means that the data is not uniformly distributed. This test computes how large the resultant vector length R must be to indicate a non-uniform distribution.

The p-value under the Rayleigh test is calculated by **Equation 10**.

$$p = \exp [\sqrt{1 + 4N + 4(N^2 - R_n^2)} - (1 + 2N)] \quad \text{Eq. 10}$$

With,

$$R_n = R * N \quad \text{Eq. 11}$$

3.3 Results

3.3.1 Signals preprocessing, QRS detection and spectrograms

After applying a bandpass filter between 0.5 and 60 Hz to remove artifacts in the ECG, the signals were examined manually to assess if significant motion artifacts were still present. In the cases where motion artifacts were present, those sections with the motion artifacts were removed from the ECG signals. After QRS complex detection in the ECG segments without motion

artifacts, those signals were concatenated, and interpolation was performed replacing the missing data with random data with the same mean and variance. **Figure 6** shows a sample of an ECG signal from one of the subjects, with the respective HRV signal obtained from QRS complex detection

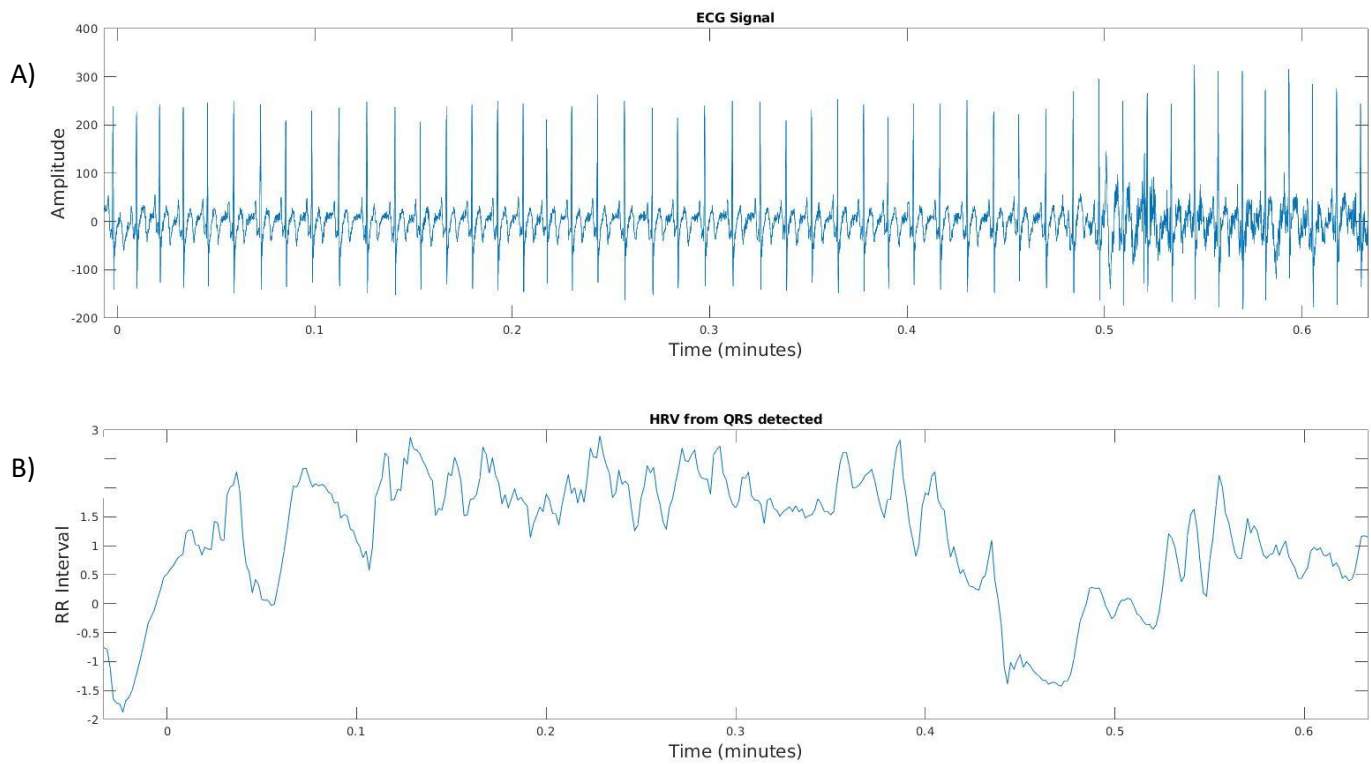


Figure 6: Extract of ECG signal from one subject

- A) ECG signal was bandpass filtering
- B) Corresponding HRV signal

The HRV signals were subtracted by their mean and divided by their standard deviation before being run through the time varying MVAR model, which then computed their spectrograms. **Figure 7** show two of the spectrograms obtained from the MVAR model. For all subjects, most of power of the signal was concentrated in the LF component.

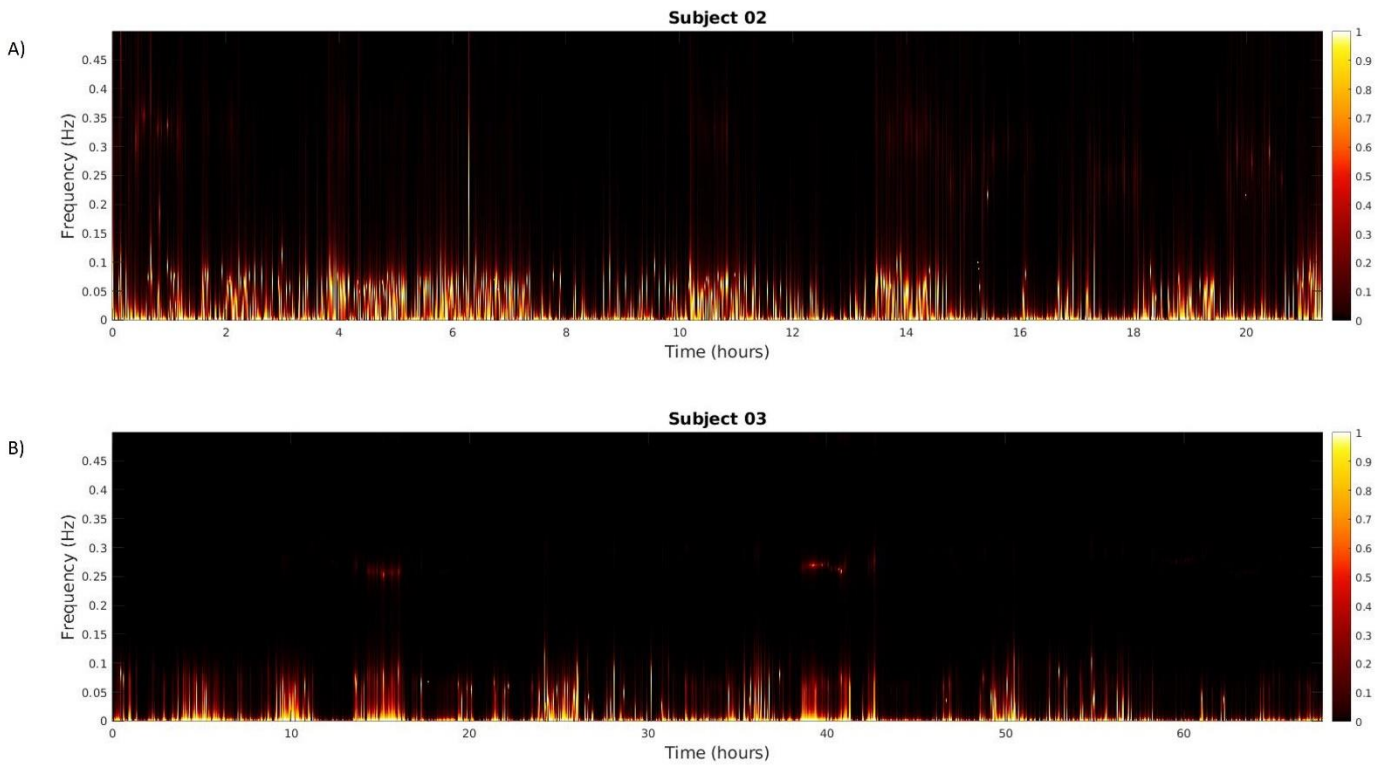


Figure 7: Spectrograms of HRV computed from two of the subjects

- A) Spectrogram of Subject 02 (21 hours)
- B) Spectrogram of Subject 03 (67 hours)

From the spectrograms, examples of the derived HF and LF bands can be seen for those two subjects in **Figure 8**, as well as the equidistant HRV signal obtained from the MVAR model.

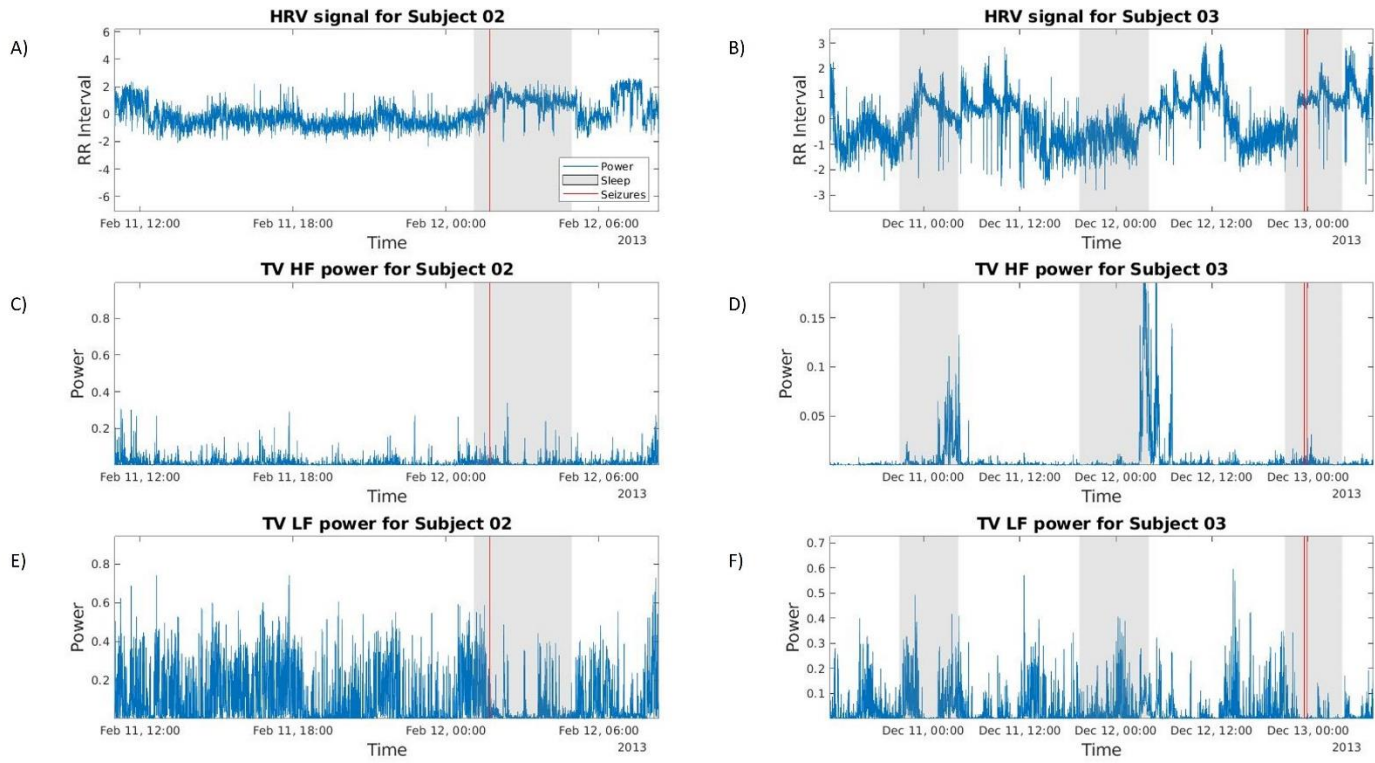


Figure 8: Examples of the three-time series derived from the MVAR model for two of the subjects

A) and B) correspond to the HRV signal with its equidistant points.

C) and D) correspond to the HF band obtained from the spectrogram.

E) and F) correspond to the LF band obtained from the spectrogram.

3.3.2 Detection of periodic components

The periodogram was computed for the three-time series of each subject. The square root of the power obtained was plotted against the inverse of the frequency. **Figure 9** shows the three periodograms obtained for subject 03. Peaks in these periodograms were used to estimate the periodic components of the signals. **Table 3** shows a summary of all the detected periodic components across the three-time series for all subjects. Significant periodicities at the group

level were deemed to be the one sixth of the circadian periodicity (around 4 hours), the half-circadian periodicity (around 12 hours) and the circadian periodicity (around 24 hours). The exact hour that these components occur varied in some instances, however, this was expected due to inter subject variability.

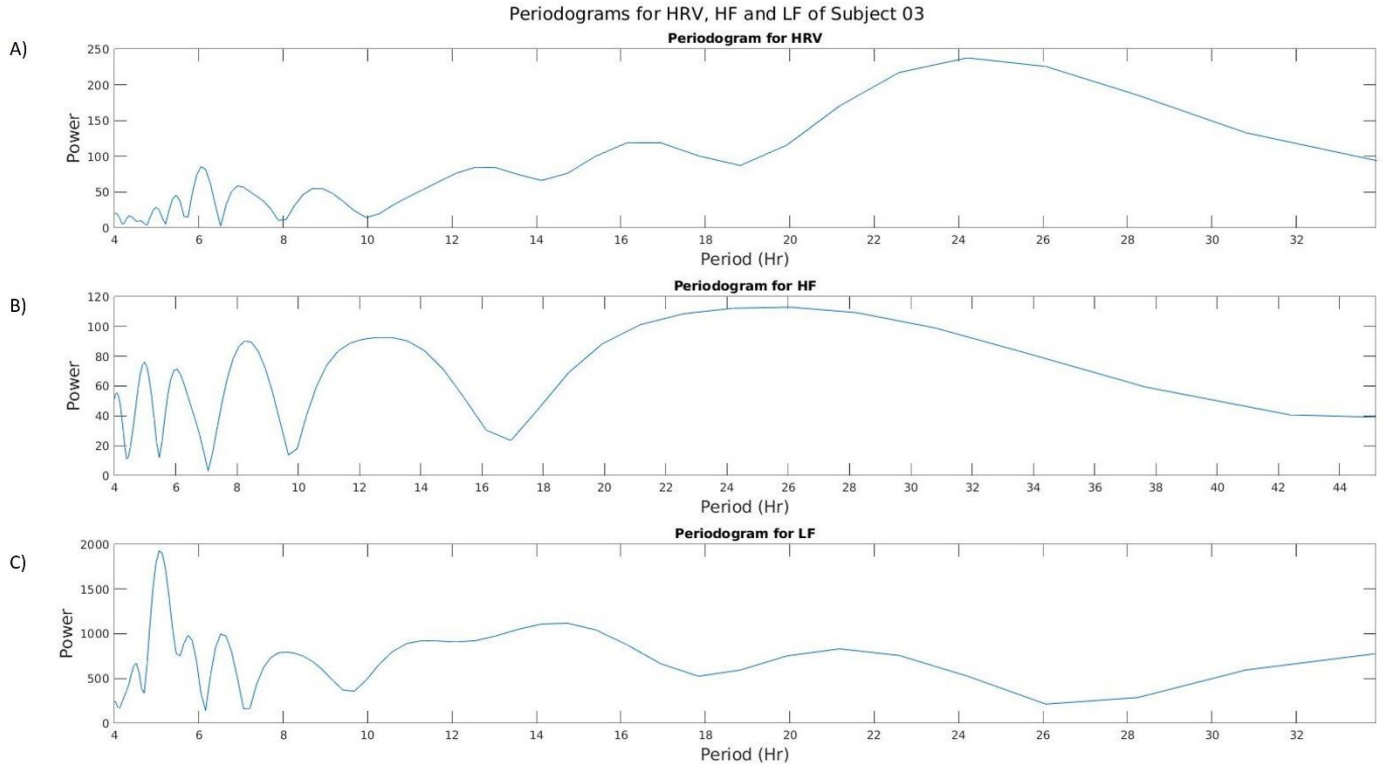


Figure 9: Periodograms obtained for subject 03

- A) Periodogram for the HRV signal.
- B) Periodogram for the HF time-varying power.
- C) Periodogram for the LF time-varying power.

SUBJECT	RECORDING LENGTH (HOURS)	HRV PERIODICITIES (HOURS)	HIGH-FREQUENCY PERIODICITIES (HOURS)	LOW-FREQUENCY PERIODICITIES (HOURS)
1	69	24	4,12,24	4, 12, 24
2	21	5, 20	4, 10,14	4, 7, 10
3	67	6, 24	4,5,8,12, 24	5,8,14,22
4	22	12, 15	3, 13	3,13
5	66	4, 24	4, 24	8, 24
6	45	4, 28	4, 12, 24	4, 12, 24
7	27	16, 19	6, 11	6, 11
8	24	12	3, 7	3, 7

Table 3: Detected periodicities for each subject in Part I

3.3.3 Filtered periodic signals and seizure correlations

Once the periodic components were identified, the three time-series were band passed filtered to extract the periodic signals and then compute the correlation of periodicities with seizure onset. **Figure 10** shows three of those filtered periodic signals for some of the most common detected periodicities. **Table 4** shows the p-values obtained from performing the Rayleigh test after computing correlation with seizure onset with significant periodicities of 4, 12 and 24 hours. **Table 5** shows the respective length of the resulting length vectors, R. A significant correlation between seizure onset and periodic signals were found for the 24-hour LF signal and for the 12-hour HF signal.

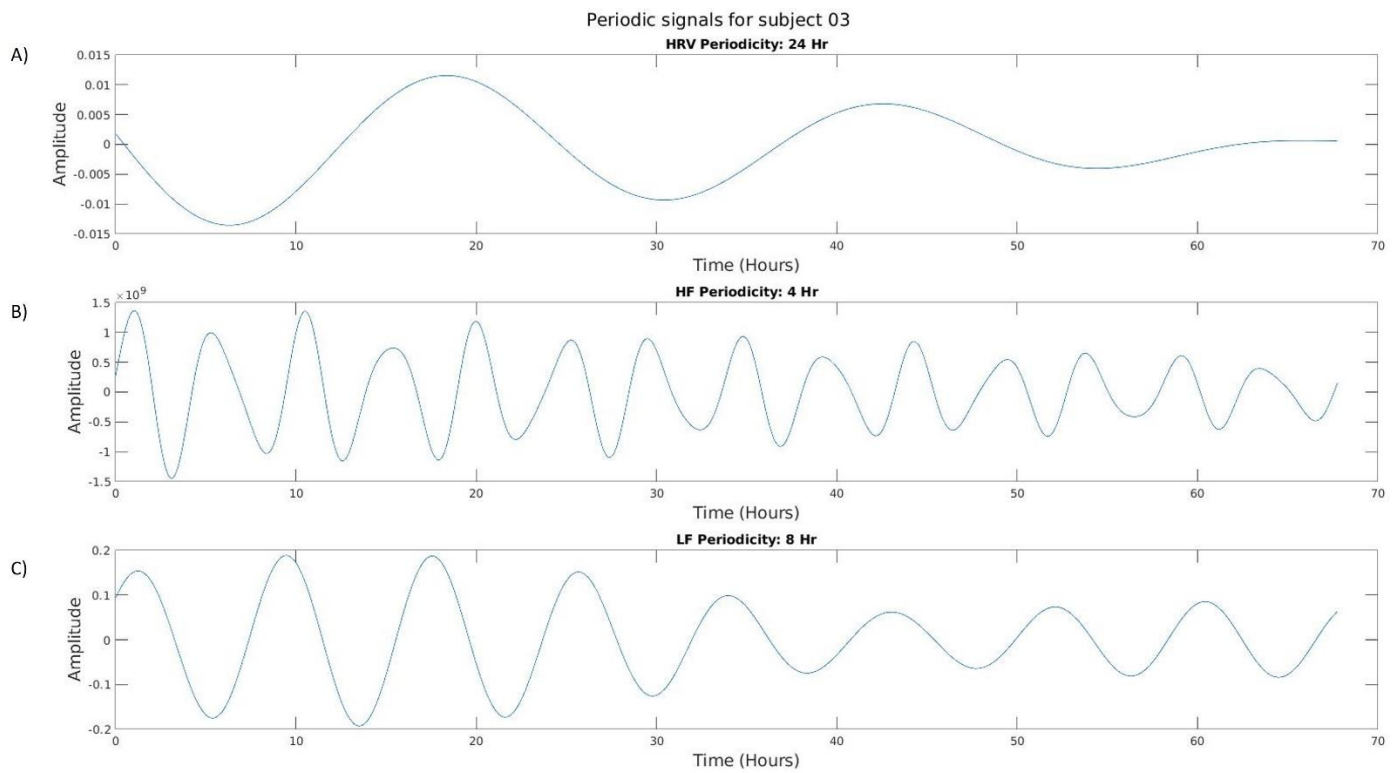


Figure 10: Examples of the filtered periodic signals from subject 03

- A) The filtered circadian periodicity of the HRV signal.
- B) The filtered four-hour periodicity for the HF signal.
- C) The filtered eight-hour periodicity for the LF signal.

P-VALUES

	HRV	HF	LF
24 HOURS	0.3270	0.4265	0.0130
12 HOURS	--	0.0140	0.2721
4 HOURS	0.3821	0.1193	0.0867

Table 4: p-values from Rayleigh test

R VALUES	HRV	HF	LF
24 HOURS	0.3223	0.3126	0.5273
12 HOURS	--	0.5410	0.3068
4 HOURS	0.409	0.4604	0.549

Table 5: R value obtained from angular plots

Figure 11 shows the angular plot and histogram distribution for the statistically significant correlation between the 24-hour periodicity and the LF signal and the also the statistically significant correlation between the 12-hour periodicity and the HF signal.

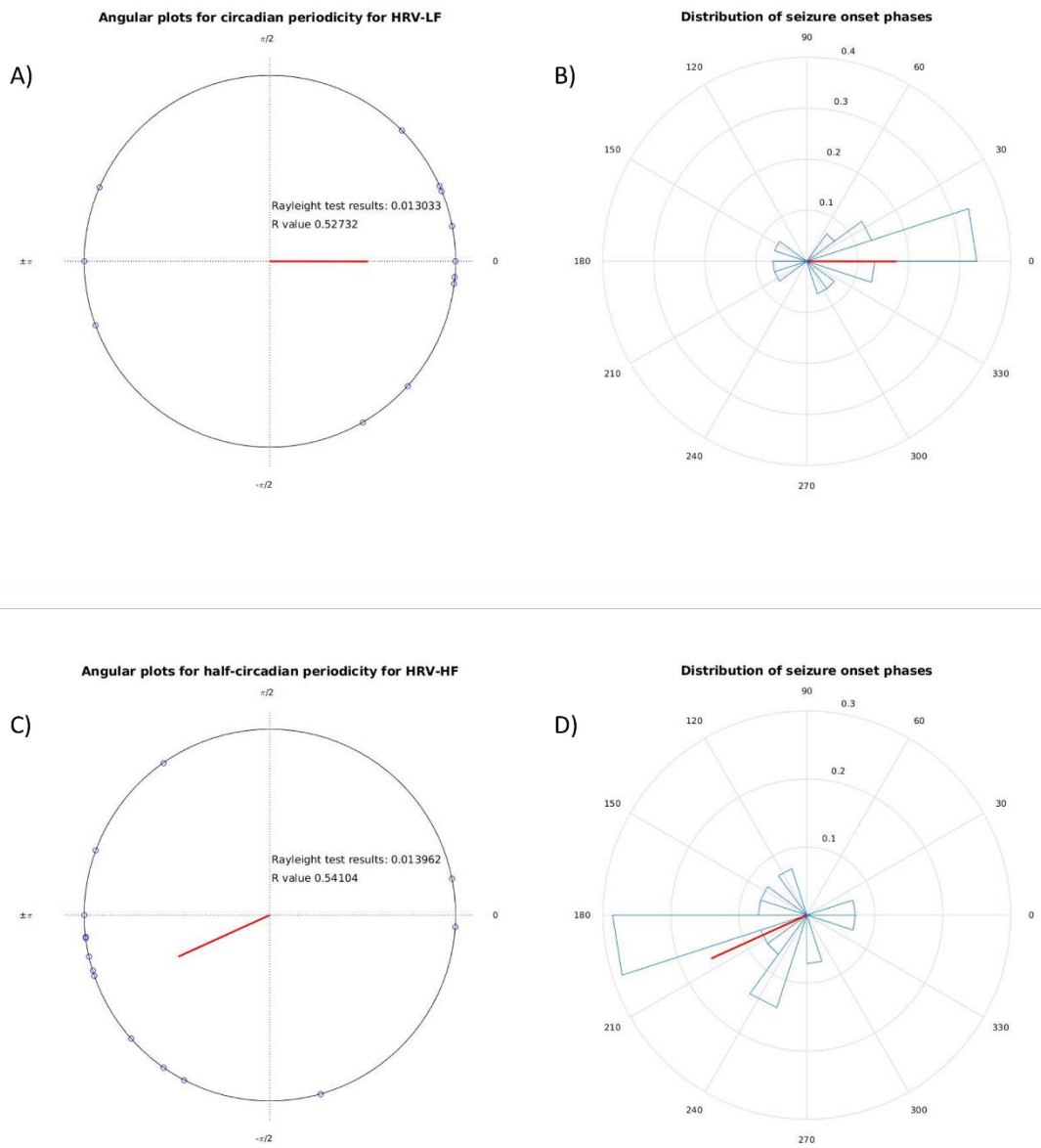


Figure 11: Angular plots for statistically significant correlations

The red lines correspond to the mean resultant vector.

- A) Position of seizure on phases of 24-hour periodic components of the LF signal. B) Respective angular histogram with phases distribution.
- C) Position of seizure on phases of 12-hour periodic components of the HF signal
- D) Respective angular histogram with phases distribution.

Chapter 4: Research Part II – Long Term Brain Heart Interactions in Epilepsy

4.1 Preface to Research Part II

In order to accomplish the general and specific objectives for Part II, the ECG and iEEG signals first were processed separately. The ECG was processed using the same methodology as in Part I. For the HRV analysis, the focus was on the LF power over time as it has been seen that the LF band is more prominent in subjects with epilepsy. For the iEEG signals, the processing scheme was done separately for each one of the frequency bands. **Figure 12** details the processing scheme that was used.

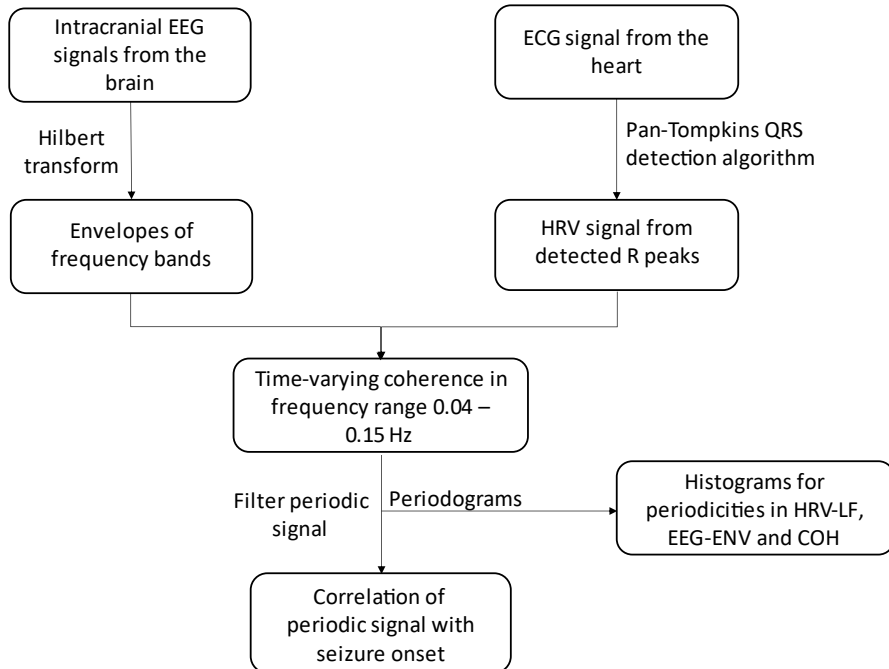


Figure 12: Processing scheme research part II

4.2 Methods

4.2.1 Envelope of iEEG signals

The first step was computing the envelope of the iEEG frequency bands. The envelope corresponds to the boundary within which the signal is contained. The purpose of computing the envelope was to have a representation of the signal that has a similar frequency range as the HRV signal of the heart [46].

In order to achieve this, first the iEEG signal was down sampled to 256 Hz, preprocessed to remove artifacts, then the 5 EEG frequency bands were extracted and then their envelope was computed using **Equation 12**. The frequency bands used correspond to the following: Delta band (1-4 Hz), Theta band (4 – 8 Hz), Alpha band (8 - 13 Hz), Beta band (13 – 30 Hz), and Gamma band (30 – 80 Hz) [57].

$$env(t) = \sqrt{x_{BP}^2 + H^2[x(t)]} \quad \text{Eq. 12}$$

With x_{BP} being the band-passed filtered iEEG frequency band and $H[x(t)]$ being the Hilbert transform of that same signal.

4.2.2 Coherence

Once the envelope of the EEG frequency bands was obtained, the QRS detection algorithm was used to detect the R peaks in the ECG signal and build an HRV time-series. Then, the two time-series has their mean subtracted, were divided by their standard deviation, and run through the MVAR model that computes the time-varying power, as well as the coherence between the two signals.

The coherence was computed using **Equation 13**.

$$COH(f, t) = \frac{S_{xy}(f, t)}{\sqrt{S_{xx}(f, t)}\sqrt{S_{yy}(f, t)}} \quad \text{Eq. 13}$$

With S_{xy} being the cross spectra between the envelope of the EEG band and the HRV of the ECG, S_{xx} and S_{yy} being the spectral power density matrices of the envelope and of the HRV.

4.2.3 Periodicity Estimation

To estimate the periodicities, first their autocorrelation was computed and then the FFT was used to obtain a periodogram for each time-series, for each subject.

An average periodogram across all subjects was then calculated for the HRV-LF, for each EEG-ENV, and for each time-varying coherence. This was done in order to obtain a clearer view of where the longer periodicities exist across all the subjects with their wildly varying length. The periodograms were computed through various methods, however, the FFT of the autocorrelation method was chosen due to the fact that by selecting a window around the zero lag of constant length across subjects it made it possible to average out across subjects with different recording lengths. Before computing the average periodogram, the periodograms obtained for each subject were normalized.

4.2.4 Correlation with seizure onset

Correlation with seizure onset was computed both at the group level and an individual level. The fact that most subjects contain various seizures allows to assess whether seizure onset correlates with the specific periodic components that were detected, a step that could not be performed in Part I. Correlations at the group level were performed by pooling together the seizures from all the subjects.

The correlation of the filtered periodic signals with seizure onset was performed in the same way as in Part I, computing the p-value through the Rayleigh test using **Equation 10**.

After computing the correlation at the group level, in order to look at how subjects with drastically more seizures could bias the results, a bootstrap-based method was used. The number of seizures from the subject who had the least amount of seizures onset were noted (8 seizures), and a random selection of that number of seizures was obtained from each subject. The correlation of periodic components with seizure onset was calculated 100 times, with a different sampling of eight seizures per subject, for a total of 96 seizures per iteration.

4.3 Results

4.3.1 Brain-heart interactions for all the frequency bands

First, the envelope was computed for the iEEG signals of each frequency band. **Figure 13** shows a sample of the envelopes computed from the iEEG signal that was used for the periodicity and coherence analysis.

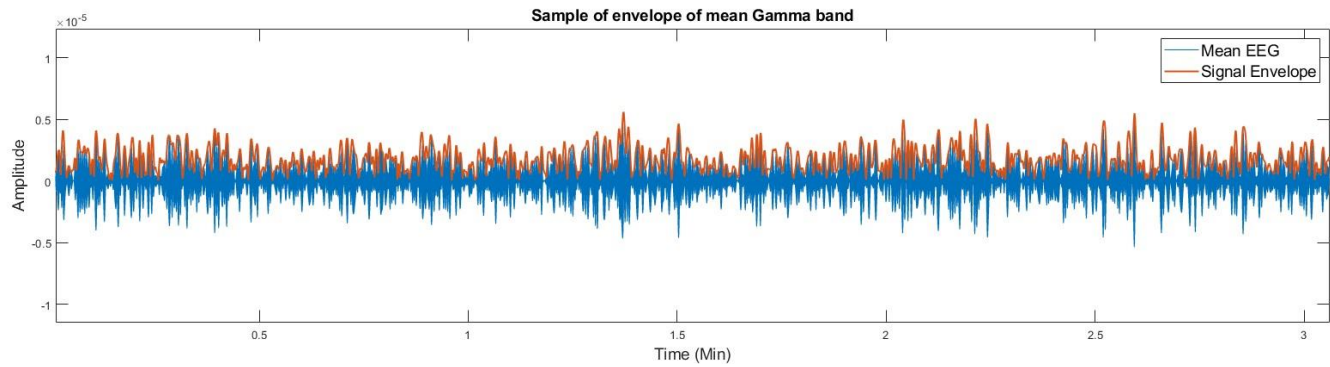


Figure 13: Extract of the Envelope computed for Gamma envelope of EEG band of subject 07

The HRV signal obtained from the ECG and then iEEG-ENV signals were z-scored and used as input for the MVAR model to obtain the power over time, then the coherence was computed. For each subject eleven time-series were obtained: HRV-LF, one for each of the envelopes of the brain bands, one for each time-varying coherence between HRV-LF and each EEG envelope. **Figure 14** shows three of those signals for one of the subjects with the time of seizure onset marked.

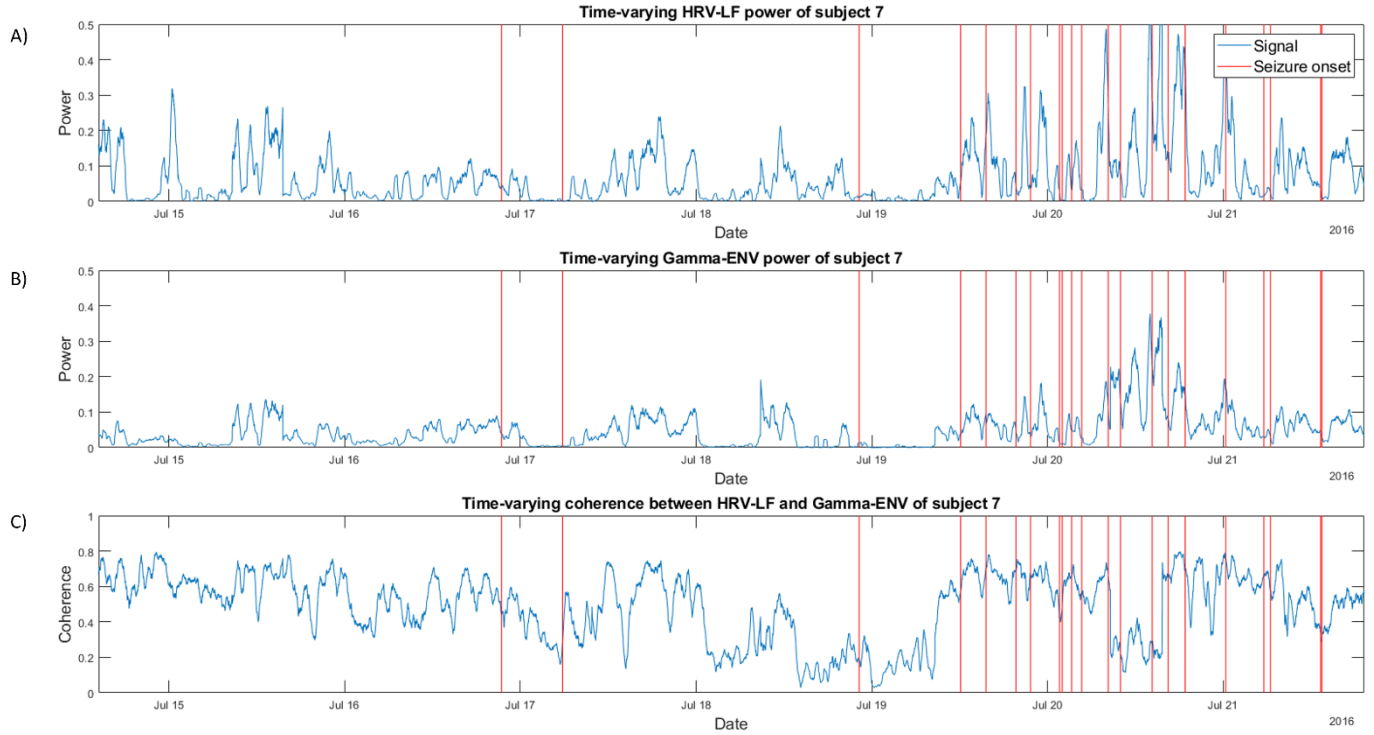


Figure 14: Time series used in Part II.

A) Power over time for HRV-LF.

B) Power over time for Gamma-ENV.

C) Power over time for coherence

In **Figure 15** the coherences for the five different brain frequency bands can be seen for this same subject. These were further smoothed out for the purpose of being able to compare more easily between the frequency bands. The coherences for all the subjects are in **Appendix A.**

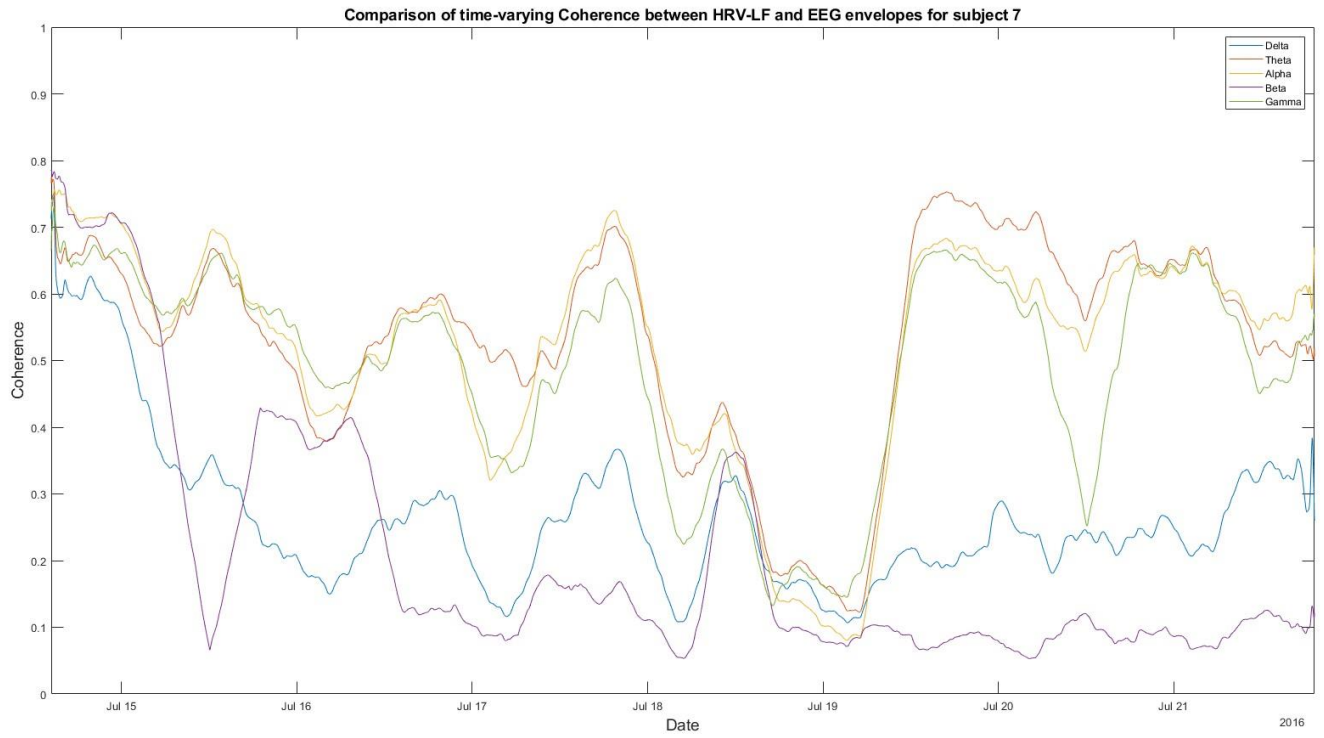


Figure 15: Time-varying coherence between HRV-LF and each EEG-ENV

4.3.2 Detection of periodic components

In order to detect the periodic components in the signals, their autocorrelation was first computed. **Figure 16** shows an example of the autocorrelations computed, which then were used to obtain the periodograms of each signal.

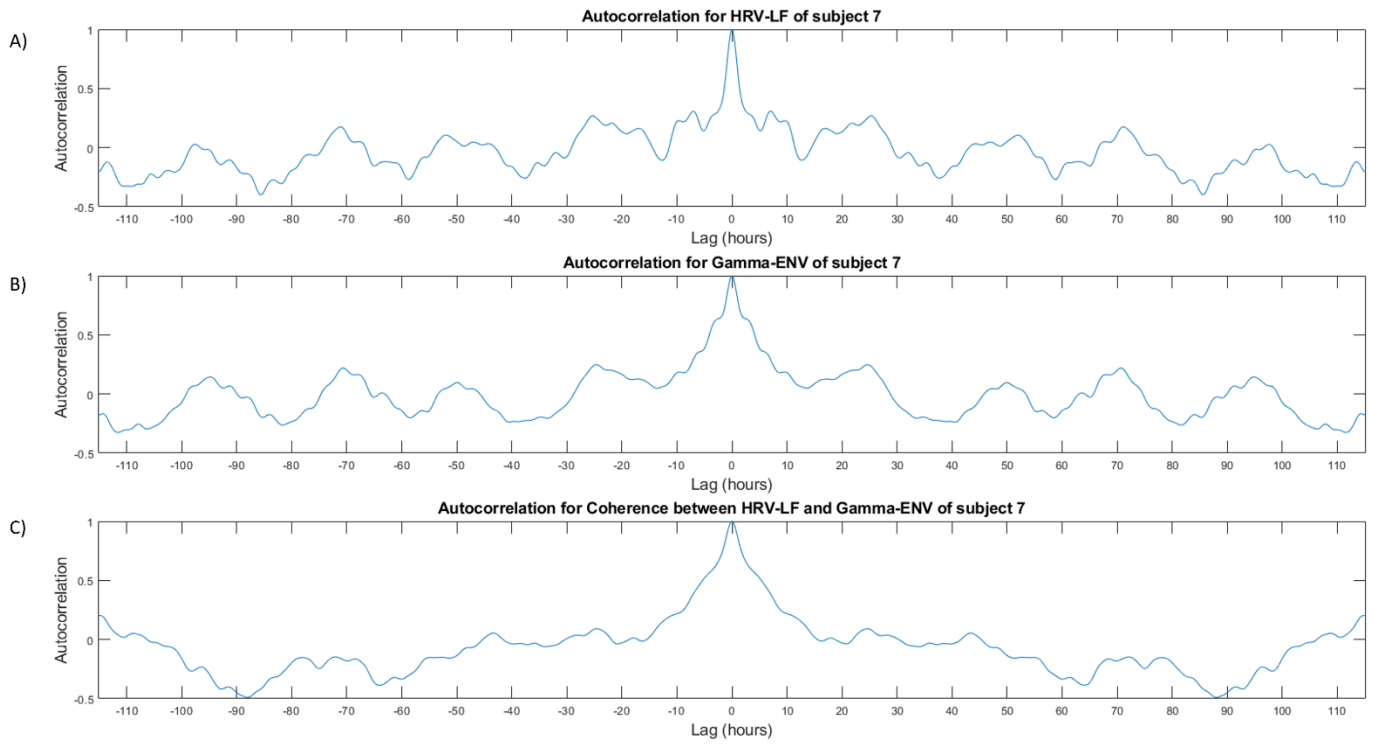


Figure 16: Autocorrelation plots for signals

- A) Autocorrelation for HRV-LF.
- B) Autocorrelation for Gamma-ENV.
- C) Autocorrelation for coherence

A consistent window around the zero lag was used to obtain the periodograms for all the signals of all subjects, the window selected -80 to 80 hours. In order to identify the periodic peaks more easily, the power was divided by the variance of the signal, then its square root was plotted in terms of the inverse of its frequency. **Figure 17** shows the periodograms of the HRV-LF, Gamma-ENV, and coherence obtained for subject seven.

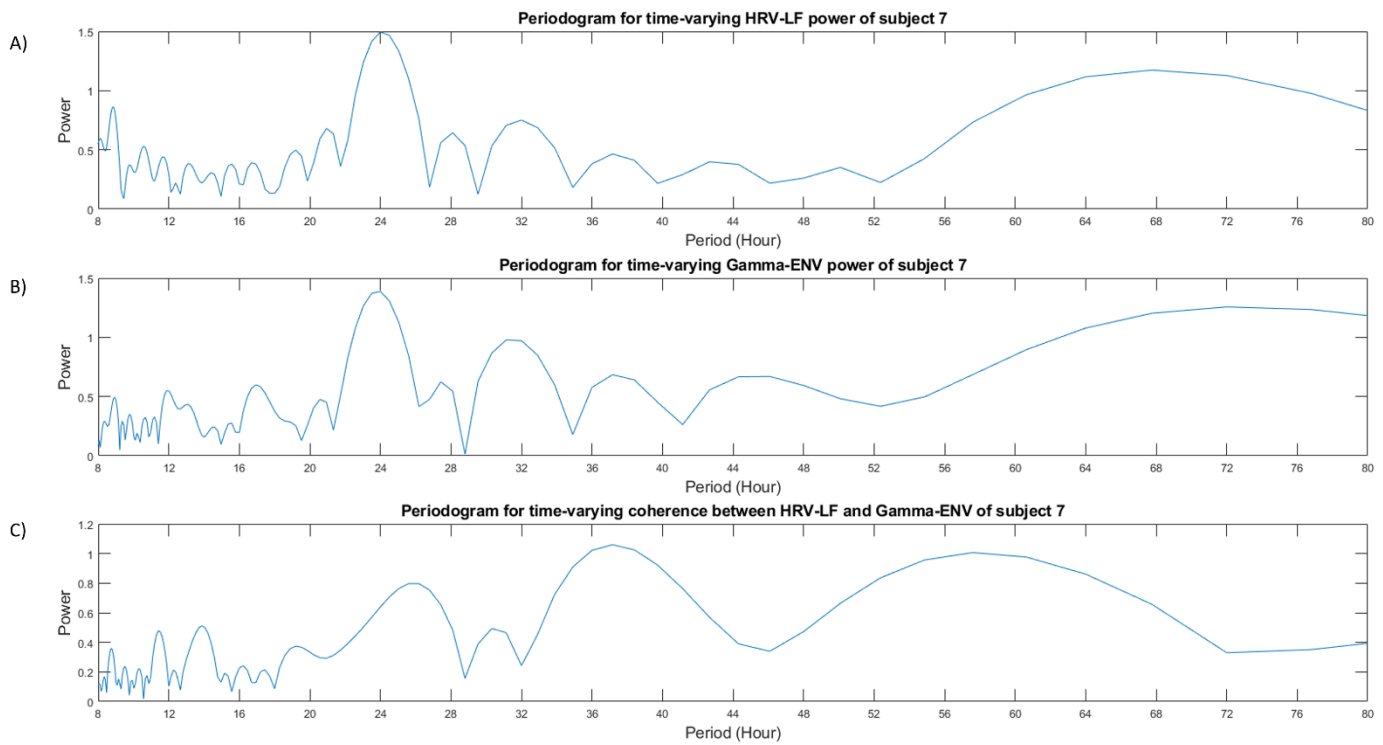


Figure 17: Periodograms for time signals

- A) Periodogram for HRV-LF.
- B) Periodogram for Gamma-ENV.
- C) Periodogram for coherence

Periodicities in signals were detected from the periodograms. In order to assess the periodic components detected across subjects, histograms were built for the detected periodic peaks and the average periodogram was computed for each signal. The histograms with the distributions of the detected periodic peaks for the HRV-LF, Gamma-ENV and coherence between those two signals can be seen in **Figure 18**. The histograms with distributions for all the other signals are in **Appendix B**.

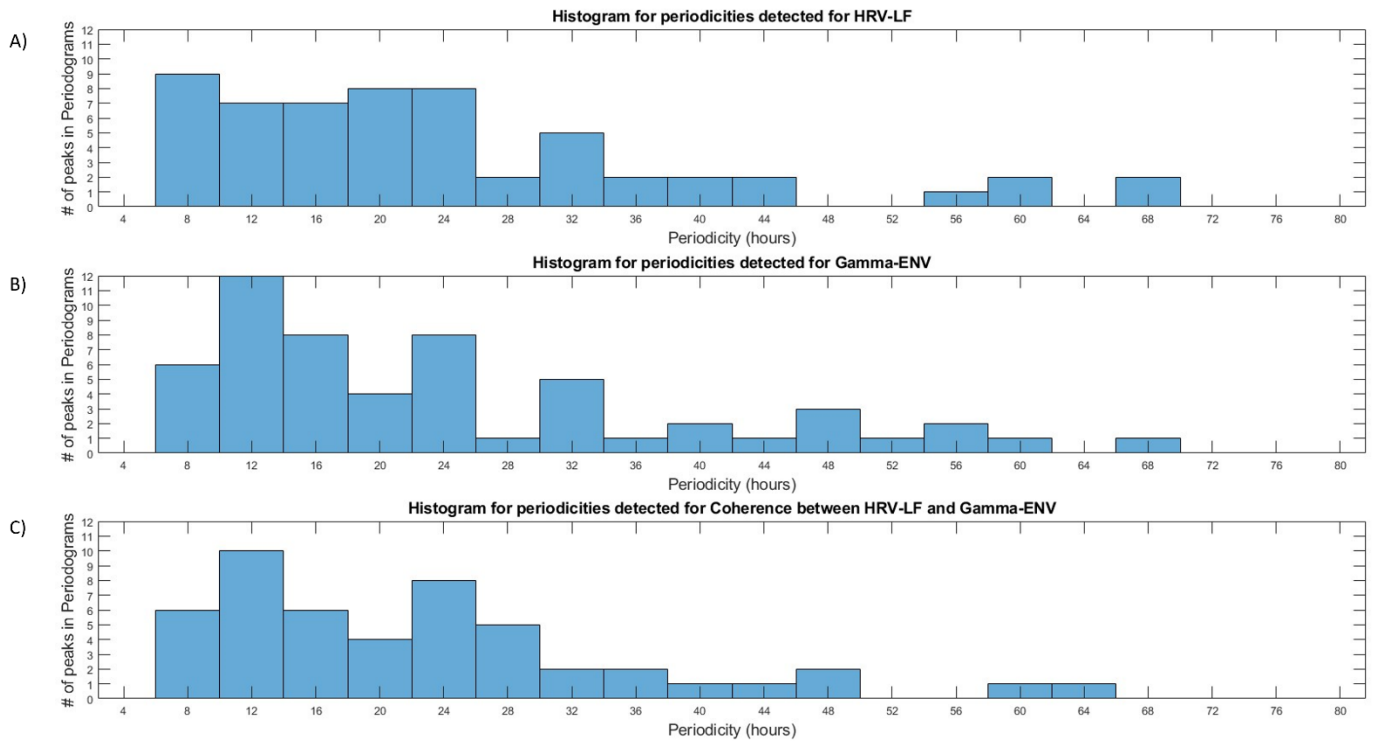


Figure 18: Histograms with distribution of periodicities detected

Only the periodicities detected above eight hours were considered for the histograms and the average periodograms due to the fact that at shorter time frames, the periodic peaks observed are less clear for various subjects.

The average periodograms were used to determine the relative strength and consistency of the periodic peaks detected across all subjects. **Figure 19** shows the average periodograms for the HRV-LF, the Gamma-ENV, and the coherence for those two signals. The average periodograms for the other signals are in **Appendix C**. The most significant periodic peaks across

all the time series were the half-circadian and the circadian one. Interestingly, for the HRV-LF signal, the crests of the periodic peaks occurred right before and after the 24 hours mark.

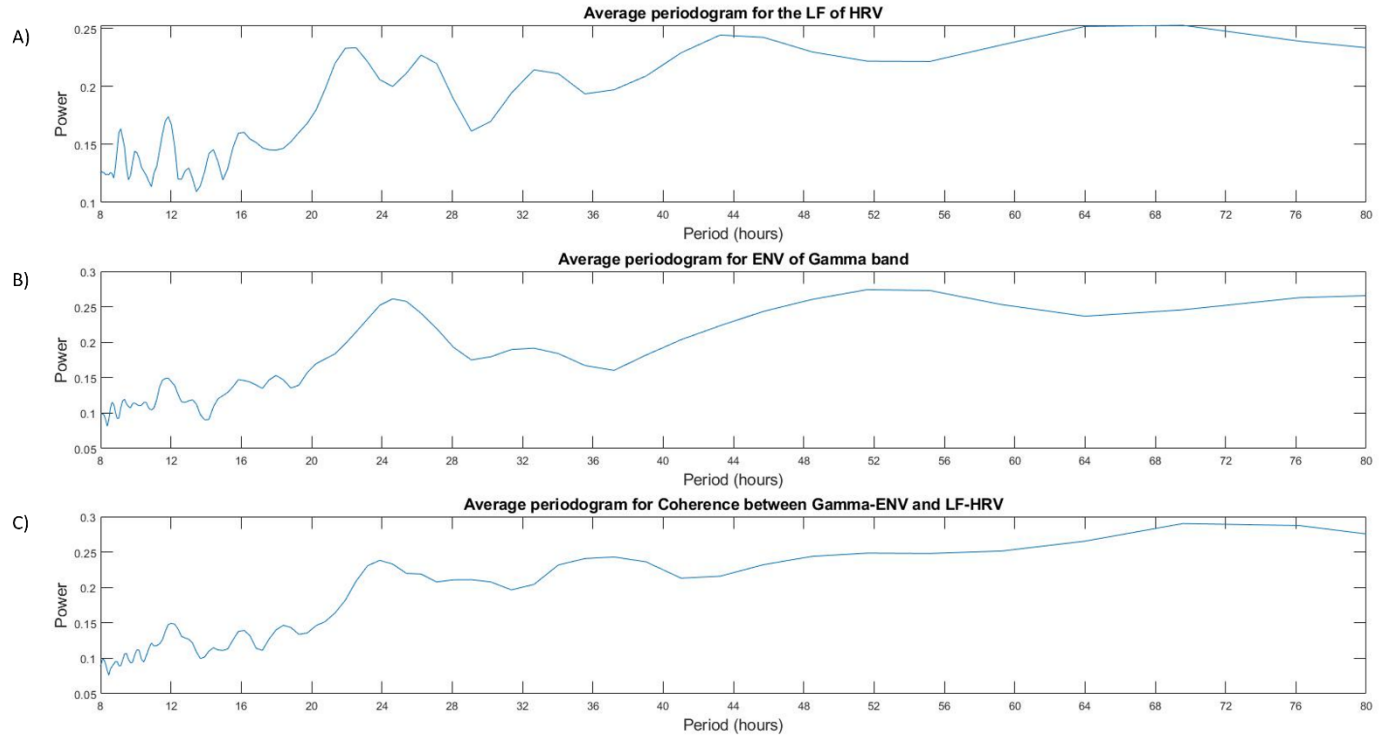


Figure 19: Average periodograms

- A) For HRV-LF.
- B) For Gamma-ENV.
- C) For coherence

4.3.3 Seizure onset correlation with periodic signals at the group level

For analyzing whether seizure correlation the circadian and half-circadian periodicities were considered, as those two periodic components were the most consistent across subjects. The phases at time of seizure onset were pooled together for all subjects and correlation with seizure onset was calculated using circular statistics. When filtering out the periodic components out of each signals, the specific period where the peaks was seen was used. **Table 6** shows the results of the Rayleigh test with the corresponding the mean resultant vector length for the signals. **Figure 20** shows the angular plots for the pooled seizure correlation analysis for the circadian periodicity of three of the time series.

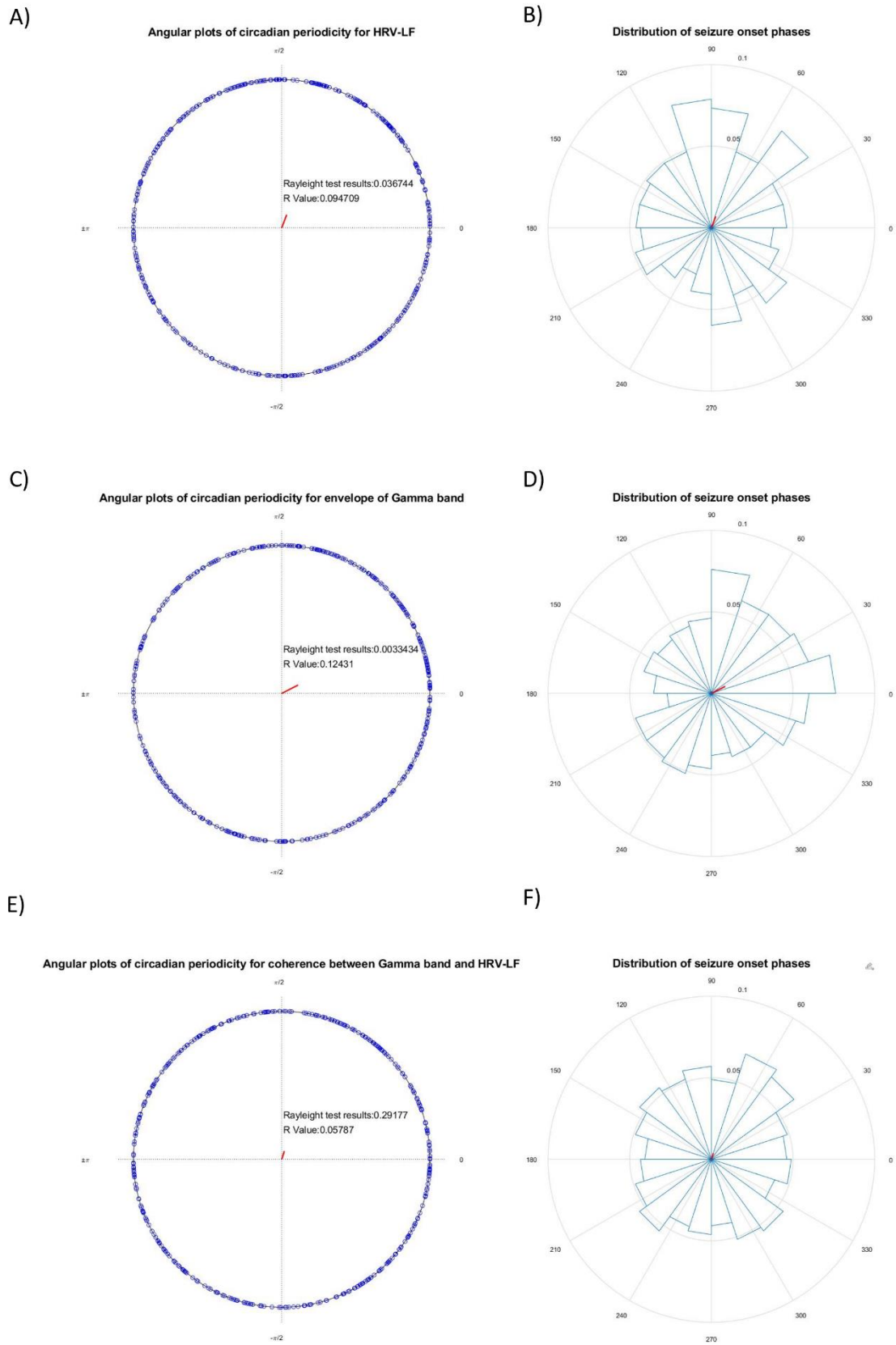


Figure 20: Angular plots for three circadian periodicities seizure correlation analysis

- A) Position of seizure on phases of circadian periodic components of the HRV- LF signal.
- B) Respective angular histogram with phases distribution.
- C) Position of seizure on phases of circadian periodic components of the Gamma-ENV signal
- D) Respective angular histogram with phases distribution.
- E) Position of seizure on phases of circadian periodic components of the Gamma-cohernce
- F) Respective angular histogram with phases distribution.

SIGNAL	Circadian Periodicity		Half-circadian periodicity	
	p-value	R value	p-value	R value
HRV-LF	0.0367	0.0947	0.3060	0.0608
DELTA-ENV	0.7628	0.0268	0.5627	0.0455
THETA-ENV	0.2486	0.0615	0.2369	0.0876
ALPHA-ENV	0.8547	0.0200	0.0391	0.1071
BETA-ENV	0.0205	0.1016	0.5483	0.0399
GAMMA-ENV	0.0033	0.1243	0.6753	0.0323
DELTA-LF COHERENCE	0.0138	0.1066	0.1459	0.0832
THETA-LF COHERENCE	0.0424	0.0926	0.0932	0.1124
ALPHA-LF COHERENCE	0.1869	0.0668	0.0327	0.1100
BETA-LF COHERENCE	0.0722	0.0836	0.0352	0.0943
GAMMA-LF COHERENCE	0.2918	0.0587	0.0400	0.0925

Table 6: Correlation of seizure onset with periodic signals

As two of the subjects had considerably more seizures than the rest of them, and in one of those two subjects they were localized to short time frame, the bootstrap method was used to analyze results with less biases. **Tables 7 & 8** report the results obtained from the bootstrap analysis for the circadian and half-circadian periods respectively, where the number of times the Null hypothesis was rejects is noted for each one of the signals.

SIGNAL	p-values < 0.05	Min p-value	Max p-value	Min R value	Max R value
HRV-LF	45	0.0049	0.9705	0.0137	0.1819
DELTA-ENV	1	0.0465	0.9938	0.0085	0.1864
THETA-ENV	11	0.0169	0.8312	0.0381	0.1782
ALPHA-ENV	0	0.0890	0.9934	0.0087	0.1657
BETA-ENV	30	0.0051	0.9968	0.0060	0.2438
GAMMA-ENV	76	2.5×10^{-5}	0.1018	0.0637	0.2558
DELTA-LF COHERENCE	20	8.9×10^{-4}	0.8990	0.0349	0.2803
THETA-LF COHERENCE	83	8.1×10^{-5}	0.2583	0.1029	0.2693
ALPHA-LF COHERENCE	1	0.0393	0.9994	0.0025	0.1915
BETA-LF COHERENCE	10	0.0085	0.9967	0.0059	0.2317
GAMMA-LF COHERENCE	17	0.0049	0.9628	0.0154	0.1819

Table 7: Bootstrap results for circadian periodicity

SIGNAL	p-values < 0.05	Min p-value	Max p-value	Min R value	Max R value
HRV-LF	6	0.0367	0.9860	0.0149	0.2266
DELTA-ENV	2	0.0237	0.9891	0.0124	0.2273
THETA-ENV	13	0.0008	0.9088	0.0293	0.2501
ALPHA-ENV	6	0.0069	0.9900	0.0118	0.2615
BETA-ENV	2	0.0134	0.9886	0.0127	0.2438
GAMMA-ENV	1	0.0394	0.9997	0.0019	0.1914
DELTA-LF COHERENCE	15	0.0046	0.9989	0.0039	0.2718
THETA-LF COHERENCE	0	0.0727	0.9839	0.0121	0.1529
ALPHA-LF COHERENCE	16	0.0008	0.9953	0.0081	0.3108
BETA-LF COHERENCE	21	0.0023	0.9913	0.0111	0.2888
GAMMA-LF COHERENCE	10	0.0001	0.9907	0.0103	0.3174

Table 8: Bootstrap results for half-circadian periodicity

4.3.4 Seizure onset correlation at the individual level

The correlation of seizure onset to the filtered periodic signals was also computed on an individual basis. For each subject, the main periodicities were obtained and the angular plots with constructed with the phases at time of seizure onset for each of the signals. **Figure 21** shows the filtered periodic signal of the HRV-LF of one of the subjects for the circadian period with the respective angular plots.

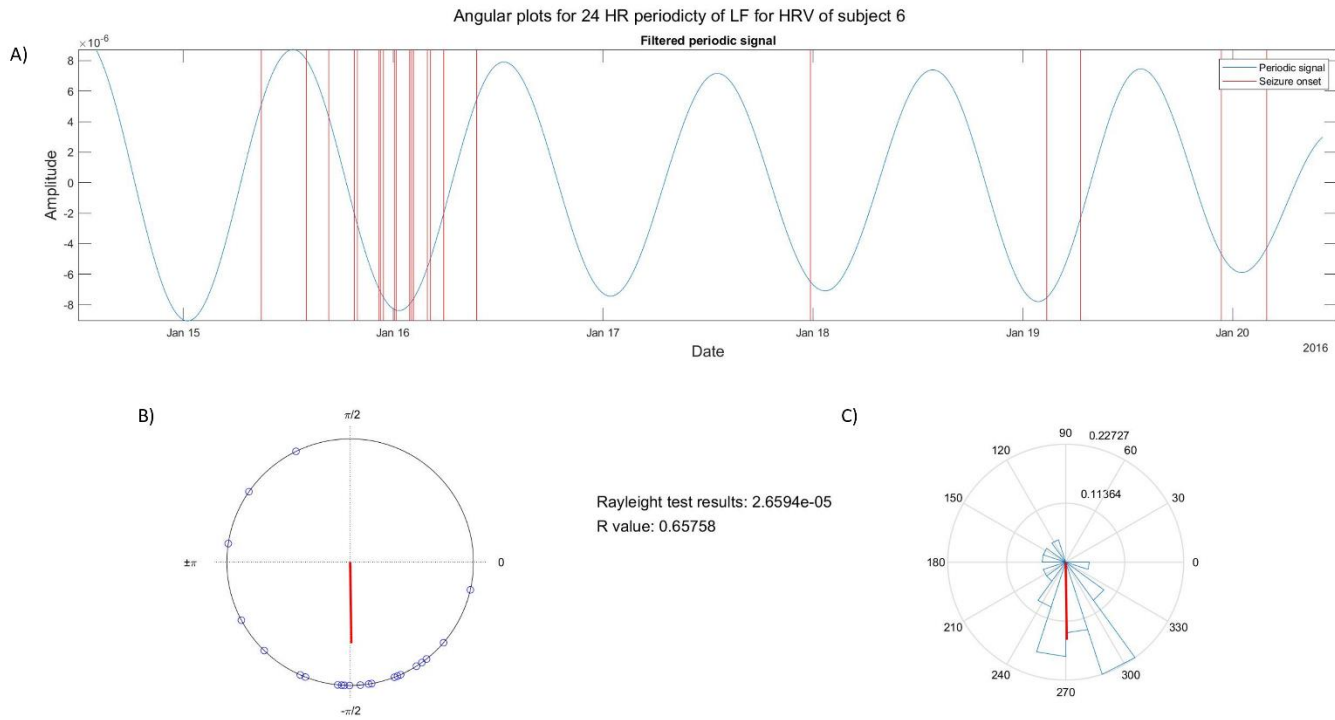


Figure 21: Seizure correlation for HRV-LF for subject 6

- A) Circadian filtered periodic signals.
- B) Angular plot with position of seizure onset.
- C) Phases distribution

Out of the 12 subjects, two of them had a lot more seizures than the others, with most of them being concentrated in a short time range. In those two subjects, so many seizures occurring so close to one another mean that no correlation of seizure onset was computed with the periodic signals. **Figure 22** shows the filtered periodic signals for subject ten, with the respective phase plot and distribution.

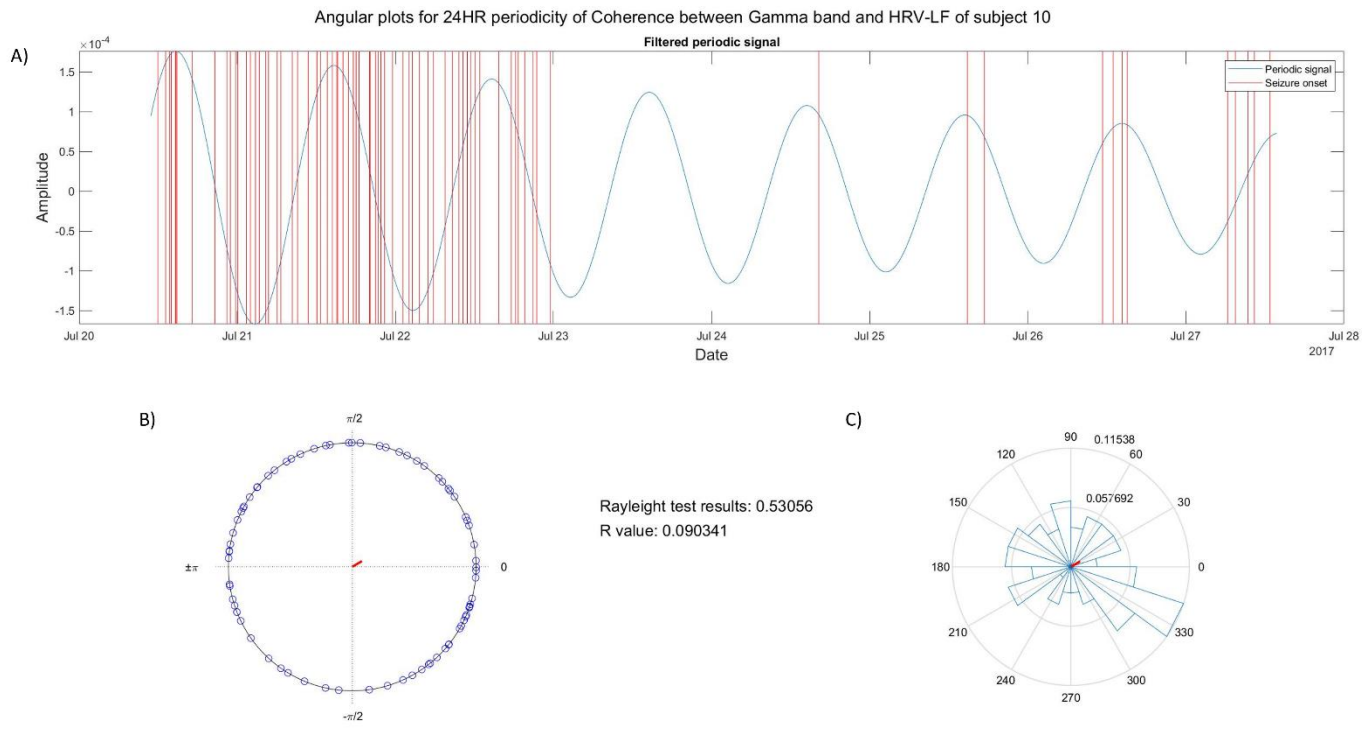


Figure 22: Seizure correlation for coherence between HRV-LF and Gamma-ENV for subject 10

- A) Circadian filtered periodic signals.
- B) Angular plot with position of seizure onset.
- C) Phases distribution

Chapter 5: Discussion

Research Part I

As seen in **Figure 7**, most of the power is concentrated among the LF part of the HRV spectrograms, with the HF power being rather low. This indicates a suppressed parasympathetic activation in the ANS, which is in accordance with previous findings. The general physiological reaction to stress in the body is the activation of the sympathetic system and the inhibition of the parasympathetic system [58]. The bodies of patients with epilepsy are under stress, and this could be fueling feedback loops that exacerbate the medical risks associated with epilepsy and thus further decreasing their quality of life even more.

Lower HF and higher LF values have been found to be predictors of cardiovascular morbidity and mortality [59], which suggests the need to take into account the ANS when studying epilepsy. Moreover, as SUDEP is theorized to be related to cardiac abnormalities, HF and LF measures could be used to assess risk that patients with epilepsy have of suffering SUDEP.

For all subjects with recordings longer than 24 hours, except for one, a circadian periodicity was found for the three time-series. This particular subject had a recording length of 27 hours, which might not have been long enough to detect a circadian periodicity. Interestingly enough, for the HRV signal, a consistent half-circadian (around 12 hours) was not detected for most subjects; however, for the HF and LF a somewhat consistent (6 out of 8 subjects) half circadian periodicity was detected. Shorter periodicities were more consistent across subjects,

with peaks around the ± 4 hours mark being detected the most often in HF (7 subjects) and LF (6 subjects). However, in the HRV signal, shorter periodicities were not seen consistently. The periodicities used in the subsequent seizure correlation analysis were chosen both because they were periods of interest and because of how consistently they were detected across subjects.

One aspect to consider about the data used in Part I is that the subjects did not have a lot of seizures during the recording time. This made individual based analysis on seizure correlation to the specific periodic components detected on the subject impossible, so the focus was only in analyzing seizure correlations on a group level.

For the correlation of the periodic components with seizure onset, the two statistically significant results were with the circadian periodicity of the LF component of the HRV, and the half-circadian periodicity of the HF component of the HRV (**Table 4**). For the HRV signal itself, no correlation was found. As the measurements that are used as a proxy of the ANS are the HF and LF power and not the HRV signal itself, it needs to be stated that the cardiac changes that are present due to seizure onset are due to disruptions in the ANS and that establishing a direct link between seizure onset and the cardiac system is not a straightforward task.

As the HF component of the HRV is tied to parasympathetic activation only, which in turn is more active in specific times of the day such as in periods of rest, it can be seen why seizure onset would correlate more strongly with the half-circadian periodicity instead of the full circadian one. The fact that the periodic circadian LF signal correlates with seizure onset could indicate that epileptic seizures tend to occur in conjunction with the parasympathetic and sympathetic systems interacting at a specific time of the day. Other studies also suggest that

epileptic seizures tend to occur at specific times of the day [10, 60]. While that time of the day seems to be particular for each subject, incorporating the information that they are more likely to have a seizure in a specific time of the day could potentially greatly increase the accuracy of seizure detection and prediction algorithms.

Overall, this study accomplished in showing how including information about the long-term biological rhythms could be beneficial when attempting to study epileptic seizure onset. Its main drawback was the limited number of seizures being considered, as well as the fact that some of the subjects in the dataset had recording lengths that made it hard to distinguish the circadian periodicities.

Research Part II

The coherence between the EEG envelopes and the HRV-LF varies substantially for each subject. By visually inspecting them (**Figure 15 and Appendix B**) it can be seen that the coherence patterns for different brain frequency bands seem to be coupled strongly to each other. The values ranged quite significantly between a minimum of around 0.05 and a maximum of approximately 0.8, with a coherence value of 1 indicating that the signals are perfectly coupled. These values are in accordance with the coherence value reported by the one other study that analyzed long term brain heart interactions in epilepsy using coherence, the caveat being that the study in question looked at coherence with the delta band only [46].

Among all the bands, the delta and the beta bands appear to be the ones that are the less coupled with the HRV-LF, as well as vary in time differently than the other bands. Both of the coherence profiles for those bands, do not seem to change with the same properties as with the other three bands. One reason why the coherence with the delta band computed was lower than with the other bands might have to do with the fact that subjects with epilepsy have repeatedly been found to have sleeping disorders, insomnia and overall, a lesser quality of sleep [61, 62]. The delta band is predominantly associated with sleep, and it was found that its overall power spectral density increases in subjects who are sleep deprived and/or that have sleep disorders [63, 64]. This changes in delta power could interfere with the established circadian rhythms, and thus decreasing the overall coherence computed with the HRV-LF. As for the beta band, it is predominantly associated with movement and conscious thoughts. The subjects in this dataset were hospitalized for the duration of the recordings so the relative time-varying power of the beta band may have been more affected than the other bands in this specific recording setup.

From the average periodograms (**Figure 19** and **Appendix C**) it can be seen that the coherence profiles overall have periodic peaks that less discernable than the EEG envelopes and those of the HRV-LF. The coherence of the HRV-LF with the gamma band exhibited the strongest periodic behavior, whereas the coherence with the delta and theta band exhibited the weakest. Circadian and half-circadian periodicities were detected in all signal EEG frequency bands, with 16–18-hour periodic peak being somewhat significant for most bands as well.

A bi-circadian periodicity was consistently seen in the EEG envelopes and the HRV-LF but not in the coherences. Overall, there was some significant variability at how many hours exactly

the bi-circadian periodicity exists for the different frequency bands as it did not occur constantly at double where the peak of the circadian periodicity was located.

Previous studies suggest that the EEG signal power itself does not seem to be correlated to seizure onset [10, 65]. However, those studies did not look at the role that the specific brain frequency bands play. In **Tables 6, 7 & 8** it can be seen that seizure correlation with periodic signals depends on the specific frequency band. As each of the frequency bands is more prominent in different bodily function and times of the day, by not making a distinction between the different bands, an enormous amount of information is being lost.

For the correlation of seizure onset with the circadian periodicity, interestingly enough, the envelopes of the faster bands (gamma and beta) correlate with seizure onset more strongly than the coherences of those respective bands, while for the slowest bands (delta and theta), the envelopes are not correlated but the coherences are correlated to seizure onset (**Table 6**). Whereas for the half-circadian periodicity correlation with seizure onset was weaker for the EEG bands, it was stronger for the coherence signals. As the relative power of the frequency bands changes throughout the day depending on the current state of the subject, it makes sense that for the EEG power the circadian periodicity was found to have stronger correlations. The bootstrap analysis reveals not only how much more strongly the circadian periodicity correlates with seizure onset but also how individual subjects can bias the results tremendously.

It was complicated to obtain any generalizable conclusion from the individual seizure correlation of brain and heart interactions due to the great extent of inter subject variability. However, keeping in mind an end goal of creating more accurate seizure detection/prediction

algorithms, this information would be needed. The correlation, mean resultant vector, and resultant vector length can be used to determine at what part of the oscillations the seizures are more likely to happen, thus obtaining the time of the day which a patients is the most at risk.

The results obtained in Part II are in accordance with the ones obtained in Part I. In both studies, using different datasets, a correlation between the circadian periodicity and the HJRV-LF was found. This further demonstrates that, for each patient, epileptic seizures tend to happen at a specific part of their cycle.

Chapter 6: Conclusion and Future Work

The human body is a complex apparatus with various system all interacting with each other exhibiting short- and long-term oscillating patterns. The studies performed in this thesis elucidated how some of the mechanisms in the ANS, such as these long-term biological rhythms, are involved in subjects with epilepsy and how periodicities in multiple physiological signals seem to be tied to epileptic seizure onset. More specifically the circadian and half-circadian periodicities were found to correlate with seizure onset, thus further demonstrating how the assumption that the inter-ictal state is stable is not correct and the need for including these slower rhythms when studying epilepsy.

It was also seen how the brain-heart interactions differ depending on which brain frequency band is being analyzed, and how when those interactions are looked at over many days, periodicities can be seen, albeit less predominantly than in the EEG frequency bands themselves.

Correlation of seizure onset to periodic components of brain signals also were shown to depend on which EEG band is being analyzed. As each EEG band is present in different physiological states, this signaled that epileptic seizures seem to be more tied to specific physiological conditions.

Creating robust seizure prediction algorithms is a task that is going to require many more years of research, however, being able to warn a person during which time of the day they are

statistically more likely to have seizure does not seem to be that far off. The potential health benefits and improvements to the quality of life if that is achieved could be enormous.

Since the goal is to create seizure detection and prediction algorithms are able to achieve better sensitivity, the future directions that this studies should take need to involve devising a method to detect which phase of the circadian periodicities correspond to seizure onset for each individual subject. That information would be able to be used to determine which time of the day a subject is the most likely to have an epileptic seizure.

Bibliography:

- [1] C. E. Stafstrom and L. Carmant, "Seizures and epilepsy: an overview for neuroscientists," (in eng), *Cold Spring Harb Perspect Med*, vol. 5, no. 6, p. a022426, 2015, doi: 10.1101/cshperspect.a022426.
- [2] J. I. Sirven, "Epilepsy: A Spectrum Disorder," (in eng), *Cold Spring Harb Perspect Med*, vol. 5, no. 9, pp. a022848-a022848, 2015, doi: 10.1101/cshperspect.a022848.
- [3] J. P. Karis and f. t. E. P. o. N. Imaging, "Epilepsy," *American Journal of Neuroradiology*, vol. 29, no. 6, pp. 1222-1224, 2008. [Online]. Available: <http://www.ajnr.org/content/ajnr/29/6/1222.full.pdf>.
- [4] F. Minwuyelet *et al.*, "Quality of life and associated factors among patients with epilepsy at specialized hospitals, Northwest Ethiopia; 2019," *PLOS ONE*, vol. 17, no. 1, p. e0262814, 2022, doi: 10.1371/journal.pone.0262814.
- [5] M. B. Wubie, M. N. Alebachew, and A. B. Yigzaw, "Common mental disorders and its determinants among epileptic patients at an outpatient epileptic clinic in Felegehiwot Referral Hospital, Bahirdar, Ethiopia: cross-sectional study," *International Journal of Mental Health Systems*, vol. 13, no. 1, p. 76, 2019/12/28 2019, doi: 10.1186/s13033-019-0333-4.
- [6] M. Seidenberg, D. T. Pulsipher, and B. Hermann, "Association of epilepsy and comorbid conditions," (in eng), *Future Neurol*, vol. 4, no. 5, pp. 663-668, 2009, doi: 10.2217/fnl.09.32.
- [7] T. Tomson, E. Beghi, A. Sundqvist, and S. I. Johannessen, "Medical risks in epilepsy: a review with focus on physical injuries, mortality, traffic accidents and their prevention," *Epilepsy Research*, vol. 60, no. 1, pp. 1-16, 2004/06/01/ 2004, doi: <https://doi.org/10.1016/j.eplepsyres.2004.05.004>.
- [8] M. R. Keezer, S. M. Sisodiya, and J. W. Sander, "Comorbidities of epilepsy: current concepts and future perspectives," (in eng), *Lancet Neurol*, vol. 15, no. 1, pp. 106-15, Jan 2016, doi: 10.1016/s1474-4422(15)00225-2.
- [9] S. Ramgopal *et al.*, "Seizure detection, seizure prediction, and closed-loop warning systems in epilepsy," *Epilepsy & Behavior*, vol. 37, pp. 291-307, 2014/08/01/ 2014, doi: <https://doi.org/10.1016/j.yebeh.2014.06.023>.
- [10] G. D. Mitsis, M. N. Anastasiadou, M. Christodoulakis, E. S. Papathanasiou, S. S. Papacostas, and A. Hadjipapas, "Functional brain networks of patients with epilepsy exhibit pronounced

- multiscale periodicities, which correlate with seizure onset," *Human Brain Mapping*, vol. 41, no. 8, pp. 2059-2076, 2020, doi: 10.1002/hbm.24930.
- [11] L. Glass, "Synchronization and rhythmic processes in physiology," *Nature*, vol. 410, no. 6825, pp. 277-284, 2001/03/01 2001, doi: 10.1038/35065745.
- [12] B. Schelter, H. Feldwisch-Drentrup, M. Ihle, A. Schulze-Bonhage, and J. Timmer, "Seizure prediction in epilepsy: from circadian concepts via probabilistic forecasting to statistical evaluation," (in eng), *Annu Int Conf IEEE Eng Med Biol Soc*, vol. 2011, pp. 1624-7, 2011, doi: 10.1109/emb.2011.6090469.
- [13] O. Devinsky, "Effects of Seizures on Autonomic and Cardiovascular Function," (in eng), *Epilepsy Curr*, vol. 4, no. 2, pp. 43-46, 2004, doi: 10.1111/j.1535-7597.2004.42001.x.
- [14] L. K. McCorry, "Physiology of the autonomic nervous system," (in eng), *Am J Pharm Educ*, vol. 71, no. 4, pp. 78-78, 2007, doi: 10.5688/aj710478.
- [15] J. M. Karemaker, "Autonomic integration: the physiological basis of cardiovascular variability," *The Journal of Physiology*, vol. 517, no. 2, pp. 316-316, 1999, doi: 10.1111/j.1469-7793.1999.0316t.x.
- [16] A. Silvani, G. Calandra-Buonaura, R. A. Dampney, and P. Cortelli, "Brain-heart interactions: physiology and clinical implications," (in eng), *Philos Trans A Math Phys Eng Sci*, vol. 374, no. 2067, May 13 2016, doi: 10.1098/rsta.2015.0181.
- [17] J. Sztajzel, "Heart rate variability: A noninvasive electrocardiographic method to measure the autonomic nervous system," *Swiss medical weekly*, vol. 134, pp. 514-22, 10/01 2004.
- [18] N. Ahmed and Y. Zhu, "Early Detection of Atrial Fibrillation Based on ECG Signals," *Bioengineering*, vol. 7, no. 1, p. 16, 2020. [Online]. Available: <https://www.mdpi.com/2306-5354/7/1/16>.
- [19] R. Kher, "Signal Processing Techniques for Removing Noise from ECG Signals," 2019.
- [20] F. Strasser, M. Muma, and A. M. Zoubir, "Motion artifact removal in ECG signals using multi-resolution thresholding," in *2012 Proceedings of the 20th European Signal Processing Conference (EUSIPCO)*, 27-31 Aug. 2012 2012, pp. 899-903.
- [21] S. Chatterjee, R. S. Thakur, R. N. Yadav, L. Gupta, and D. K. Raghuvanshi, "Review of noise removal techniques in ECG signals," *IET Signal Processing*, vol. 14, no. 9, pp. 569-590, 2020, doi: <https://doi.org/10.1049/iet-spr.2020.0104>.
- [22] T. F. o. t. E. S. o. C. t. N. A. S. o. P. Electrophysiology, "Heart Rate Variability," *Circulation*, vol. 93, no. 5, pp. 1043-1065, 1996, doi: doi:10.1161/01.CIR.93.5.1043.

- [23] K. Li, H. Rüdiger, and T. Ziemssen, "Spectral Analysis of Heart Rate Variability: Time Window Matters," (in English), *Frontiers in Neurology*, Perspective vol. 10, no. 545, 2019-May-29 2019, doi: 10.3389/fneur.2019.00545.
- [24] V. P. S. Naidu, "Time-Frequency Distribution of HRV Signal by Wigner-Ville Spectral Analysis in MI Patients," *IETE Technical Review*, vol. 18, no. 5, pp. 361-364, 2001/09/01 2001, doi: 10.1080/02564602.2001.11416984.
- [25] H. Rüdiger, L. Klinghammer, and K. Scheuch, "The trigonometric regressive spectral analysis—a method for mapping of beat-to-beat recorded cardiovascular parameters on to frequency domain in comparison with Fourier transformation," *Computer Methods and Programs in Biomedicine*, vol. 58, no. 1, pp. 1-15, 1998/01/01/ 1998, doi: [https://doi.org/10.1016/S0169-2607\(98\)00070-4](https://doi.org/10.1016/S0169-2607(98)00070-4).
- [26] N. Aimie-Salleh, M. B. Malarvili, and A. C. Phillip, "Quantitative Comparison of Time Frequency Distribution for Heart Rate Variability Using Performance Measure," 2015.
- [27] A. Voss, R. Schroeder, A. Heitmann, A. Peters, and S. Perz, "Short-Term Heart Rate Variability—Influence of Gender and Age in Healthy Subjects," *PLOS ONE*, vol. 10, no. 3, p. e0118308, 2015, doi: 10.1371/journal.pone.0118308.
- [28] P. A. Lotufo, L. Valiengo, I. M. Benseñor, and A. R. Brunoni, "A systematic review and meta-analysis of heart rate variability in epilepsy and antiepileptic drugs," *Epilepsia*, vol. 53, no. 2, pp. 272-282, 2012, doi: 10.1111/j.1528-1167.2011.03361.x.
- [29] M. Zijlmans, D. Flanagan, and J. Gotman, "Heart Rate Changes and ECG Abnormalities During Epileptic Seizures: Prevalence and Definition of an Objective Clinical Sign," *Epilepsia*, vol. 43, no. 8, pp. 847-854, 2002, doi: 10.1046/j.1528-1157.2002.37801.x.
- [30] L. Nashef, "Sudden unexpected death in epilepsy: terminology and definitions," *Epilepsia*, vol. 38, pp. S6-S8, 1997.
- [31] C. A. Massey, L. P. Sowers, B. J. Dlouhy, and G. B. Richerson, "Mechanisms of sudden unexpected death in epilepsy: the pathway to prevention," (in eng), *Nat Rev Neurol*, vol. 10, no. 5, pp. 271-282, 2014, doi: 10.1038/nrneurol.2014.64.
- [32] M. T. Faria *et al.*, "Heart rate variability in patients with refractory epilepsy: The influence of generalized convulsive seizures," *Epilepsy Research*, vol. 178, p. 106796, 2021/12/01/ 2021, doi: <https://doi.org/10.1016/j.epilepsyres.2021.106796>.
- [33] K. Schiecke, A. Schumann, F. Benninger, M. Feucht, K.-J. Baer, and P. Schlattmann, "Brain–heart interactions considering complex physiological data: processing schemes for time-variant,

frequency-dependent, topographical and statistical examination of directed interactions by convergent cross mapping," *Physiological Measurement*, vol. 40, no. 11, p. 114001, 2019/11/01 2019, doi: 10.1088/1361-6579/ab5050.

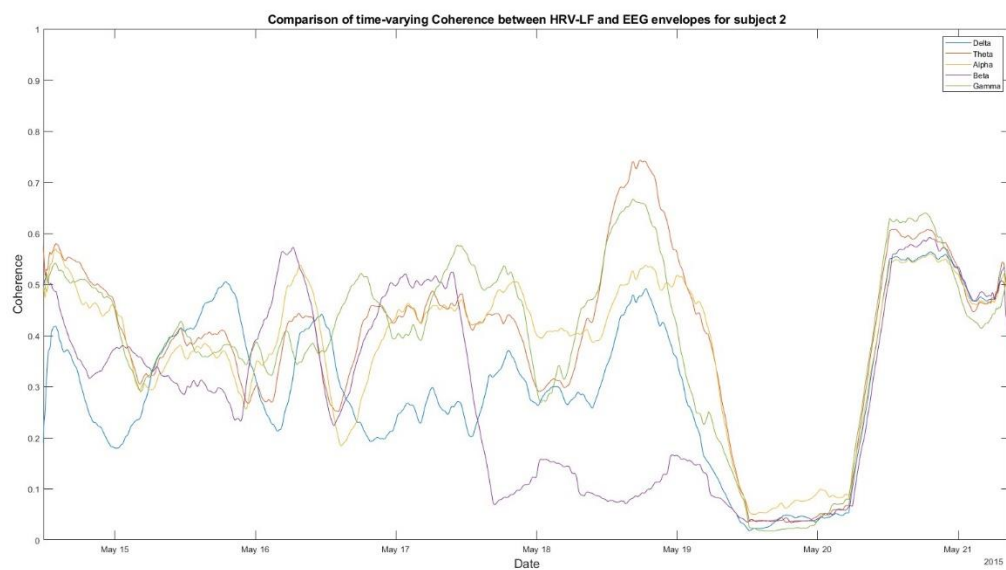
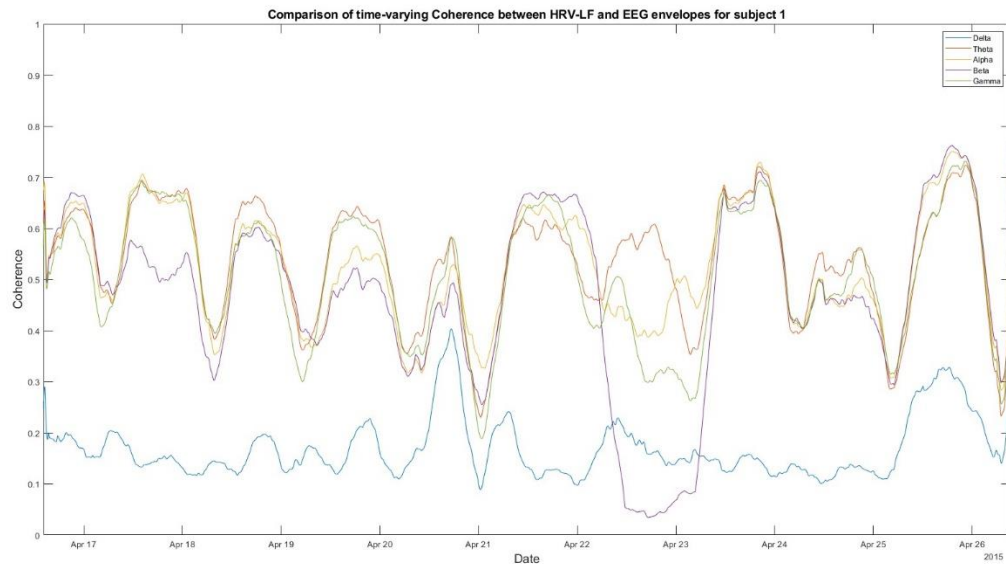
- [34] G. Valenza, N. Toschi, and R. Barbieri, "Uncovering brain-heart information through advanced signal and image processing," *Philosophical Transactions of the Royal Society A: Mathematical, Physical and Engineering Sciences*, vol. 374, no. 2067, p. 20160020, 2016, doi: doi:10.1098/rsta.2016.0020.
- [35] T. Sabatini, G. B. Frisoni, P. Barbisoni, G. Bellelli, R. Rozzini, and M. Trabucchi, "Atrial Fibrillation and Cognitive Disorders in Older People," *Journal of the American Geriatrics Society*, vol. 48, no. 4, pp. 387-390, 2000, doi: <https://doi.org/10.1111/j.1532-5415.2000.tb04695.x>.
- [36] A. Bashan, R. P. Bartsch, J. W. Kantelhardt, S. Havlin, and P. C. Ivanov, "Network physiology reveals relations between network topology and physiological function," *Nature Communications*, vol. 3, no. 1, p. 702, 2012/02/28 2012, doi: 10.1038/ncomms1705.
- [37] A. Duggento *et al.*, "Globally conditioned Granger causality in brain-brain and brain-heart interactions: a combined heart rate variability/ultra-high-field (7 T) functional magnetic resonance imaging study," *Philosophical Transactions of the Royal Society A: Mathematical, Physical and Engineering Sciences*, vol. 374, no. 2067, p. 20150185, 2016, doi: doi:10.1098/rsta.2015.0185.
- [38] F. Jurysta *et al.*, "A study of the dynamic interactions between sleep EEG and heart rate variability in healthy young men," *Clinical Neurophysiology*, vol. 114, no. 11, pp. 2146-2155, 2003/11/01/ 2003, doi: [https://doi.org/10.1016/S1388-2457\(03\)00215-3](https://doi.org/10.1016/S1388-2457(03)00215-3).
- [39] C. W. J. Granger, "Investigating Causal Relations by Econometric Models and Cross-spectral Methods," *Econometrica*, vol. 37, no. 3, pp. 424-438, 1969, doi: 10.2307/1912791.
- [40] A. K. Seth, A. B. Barrett, and L. Barnett, "Granger Causality Analysis in Neuroscience and Neuroimaging," *The Journal of Neuroscience*, vol. 35, no. 8, pp. 3293-3297, 2015, doi: 10.1523/jneurosci.4399-14.2015.
- [41] J. Yang, Y. Pan, and Y. Luo, "Investigation of brain-heart network during sleep," in *2020 42nd Annual International Conference of the IEEE Engineering in Medicine & Biology Society (EMBC)*, 20-24 July 2020 2020, pp. 3343-3346, doi: 10.1109/EMBC44109.2020.9175305.
- [42] M. Ursino, G. Ricci, and E. Magosso, "Transfer Entropy as a Measure of Brain Connectivity: A Critical Analysis With the Help of Neural Mass Models," (in English), *Frontiers in Computational Neuroscience*, Original Research vol. 14, 2020-June-05 2020, doi: 10.3389/fncom.2020.00045.

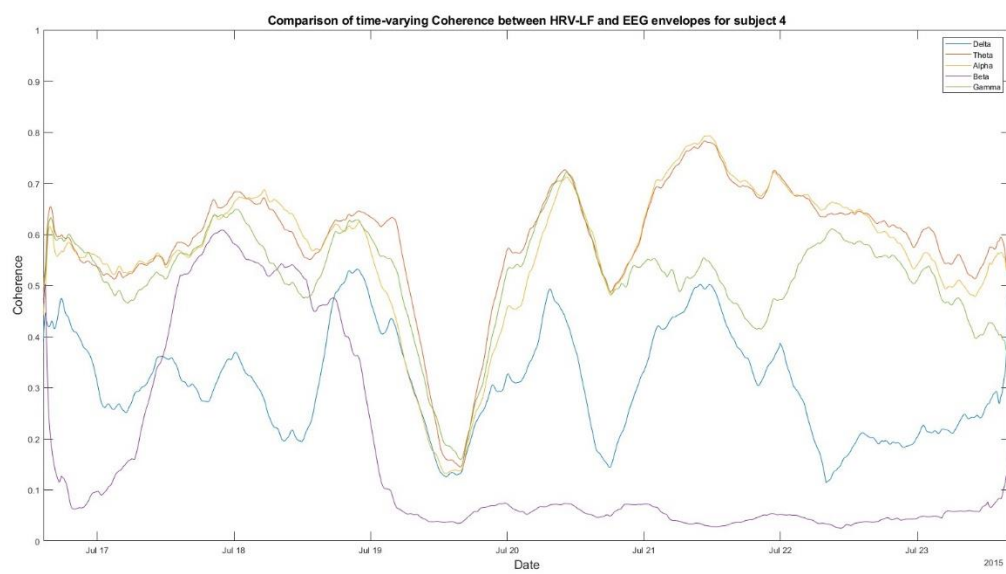
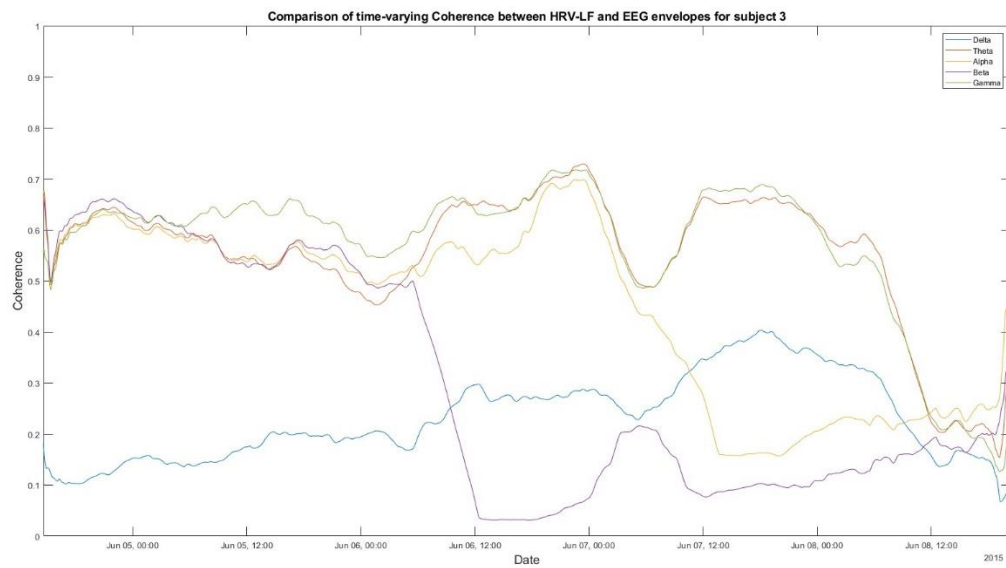
- [43] K. Yoshinaga *et al.*, "Comparison of Phase Synchronization Measures for Identifying Stimulus-Induced Functional Connectivity in Human Magnetoencephalographic and Simulated Data," (in English), *Frontiers in Neuroscience*, Original Research vol. 14, 2020-June-19 2020, doi: 10.3389/fnins.2020.00648.
- [44] R. Bruña, F. Maestú, and E. Pereda, "Phase locking value revisited: teaching new tricks to an old dog," (in eng), *J Neural Eng*, vol. 15, no. 5, p. 056011, Oct 2018, doi: 10.1088/1741-2552/aacfe4.
- [45] C. Stam and A. Daffertshofer, "Phase lag index: Assessment of functional connectivity from multi channel EEG and MEG with diminished bias from common sources," *Human brain mapping*, vol. 28, pp. 1178-93, 11/01 2007, doi: 10.1002/hbm.20346.
- [46] D. Piper *et al.*, "Synchronization analysis between heart rate variability and EEG activity before, during, and after epileptic seizure," (in eng), *Biomed Tech (Berl)*, vol. 59, no. 4, pp. 343-55, Aug 2014, doi: 10.1515/bmt-2013-0139.
- [47] M. Wacker and H. Witte, "Time-frequency techniques in biomedical signal analysis. a tutorial review of similarities and differences," (in eng), *Methods Inf Med*, vol. 52, no. 4, pp. 279-96, 2013, doi: 10.3414/me12-01-0083.
- [48] J. Parvizi and S. Kastner, "Promises and limitations of human intracranial electroencephalography," (in eng), *Nat Neurosci*, vol. 21, no. 4, pp. 474-483, Apr 2018, doi: 10.1038/s41593-018-0108-2.
- [49] S. Kovac, V. N. Vakharia, C. Scott, and B. Diehl, "Invasive epilepsy surgery evaluation," (in eng), *Seizure*, vol. 44, pp. 125-136, Jan 2017, doi: 10.1016/j.seizure.2016.10.016.
- [50] B. C. Jobst *et al.*, "Intracranial EEG in the 21st Century," (in eng), *Epilepsy Curr*, vol. 20, no. 4, pp. 180-188, Jul 2020, doi: 10.1177/1535759720934852.
- [51] M. Fahimi Hnazaee *et al.*, "Localization of deep brain activity with scalp and subdural EEG," *NeuroImage*, vol. 223, p. 117344, 2020/12/01/ 2020, doi: <https://doi.org/10.1016/j.neuroimage.2020.117344>.
- [52] J. Pan and W. J. Tompkins, "A Real-Time QRS Detection Algorithm," *IEEE Transactions on Biomedical Engineering*, vol. BME-32, no. 3, pp. 230-236, 1985, doi: 10.1109/TBME.1985.325532.
- [53] M. Hashim, Y. W. Hau, and R. Bakhteri, "Efficient QRS complex detection algorithm implementation on soc-based embedded system," *Jurnal Teknologi*, vol. 78, 07/26 2016, doi: 10.11113/jt.v78.9450.

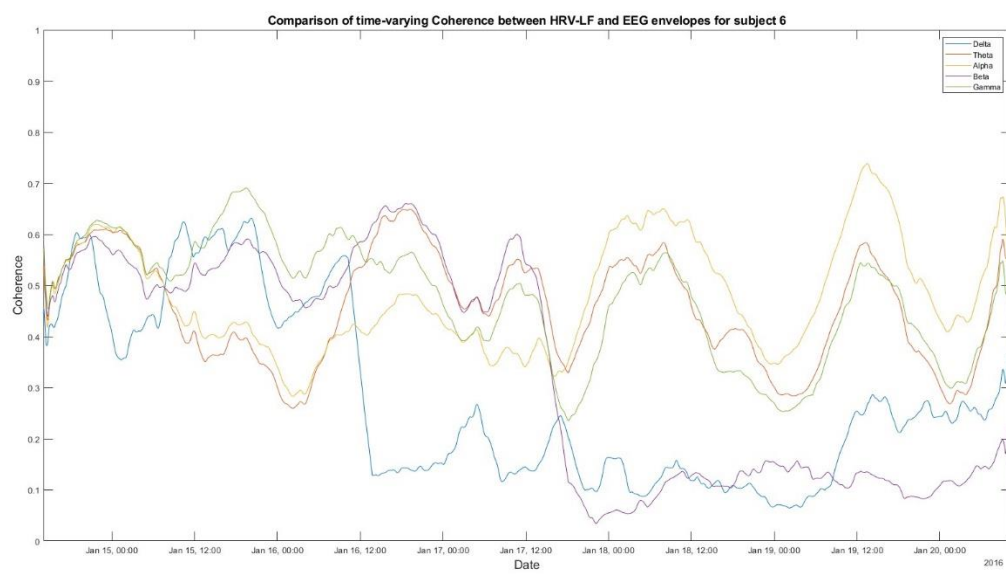
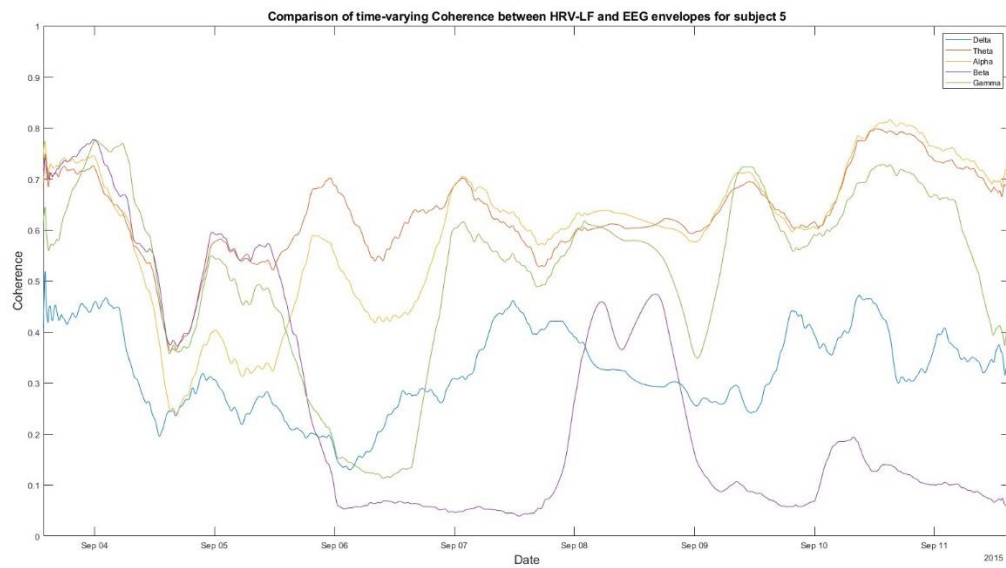
- [54] K. Kostoglou, A. Robertson, B. MacIntosh, and G. Mitsis, "A Novel Framework for Estimating Time-Varying Multivariate Autoregressive Models and Application to Cardiovascular Responses to Acute Exercise," *IEEE Transactions on Biomedical Engineering*, 03/05 2019, doi: 10.1109/TBME.2019.2903012.
- [55] A. D. Poularikas, *Transforms and applications handbook*. CRC press, 2018.
- [56] B. Philipp, "CircStat: a MATLAB toolbox for circular statistics," *Journal of Statistical Software*, vol. 31, 09/01 2009, doi: 10.18637/jss.v031.i10.
- [57] D. M. Groppe *et al.*, "Dominant frequencies of resting human brain activity as measured by the electrocorticogram," *NeuroImage*, vol. 79, pp. 223-233, 2013/10/01/ 2013, doi: <https://doi.org/10.1016/j.neuroimage.2013.04.044>.
- [58] M. G. Ziegler, "50 - Psychological Stress and the Autonomic Nervous System," in *Primer on the Autonomic Nervous System (Second Edition)*, D. Robertson, I. Biaggioni, G. Burnstock, and P. A. Low Eds. San Diego: Academic Press, 2004, pp. 189-190.
- [59] G. Ernst, "Heart-Rate Variability—More than Heart Beats?," (in English), *Frontiers in Public Health*, Review vol. 5, 2017-September-11 2017, doi: 10.3389/fpubh.2017.00240.
- [60] P. J. Karoly *et al.*, "The circadian profile of epilepsy improves seizure forecasting," (in eng), *Brain*, vol. 140, no. 8, pp. 2169-2182, Aug 1 2017, doi: 10.1093/brain/awx173.
- [61] M. Quigg *et al.*, "Insomnia in epilepsy is associated with continuing seizures and worse quality of life," (in eng), *Epilepsy Res*, vol. 122, pp. 91-6, May 2016, doi: 10.1016/j.eplepsyres.2016.02.014.
- [62] A. Jacoby, D. Snape, S. Lane, and G. A. Baker, "Self-reported anxiety and sleep problems in people with epilepsy and their association with quality of life," (in eng), *Epilepsy Behav*, vol. 43, pp. 149-58, Feb 2015, doi: 10.1016/j.yebeh.2014.09.071.
- [63] S. Long, R. Ding, J. Wang, Y. Yu, J. Lu, and D. Yao, "Sleep Quality and Electroencephalogram Delta Power," (in English), *Frontiers in Neuroscience*, Mini Review vol. 15, 2021-December-15 2021, doi: 10.3389/fnins.2021.803507.
- [64] S. Ammanuel *et al.*, "Heightened Delta Power during Slow-Wave-Sleep in Patients with Rett Syndrome Associated with Poor Sleep Efficiency," *PLOS ONE*, vol. 10, no. 10, p. e0138113, 2015, doi: 10.1371/journal.pone.0138113.
- [65] P. J. Karoly *et al.*, "Multiday cycles of heart rate are associated with seizure likelihood: An observational cohort study," *EBioMedicine*, vol. 72, p. 103619, 2021/10/01/ 2021, doi: <https://doi.org/10.1016/j.ebiom.2021.103619>.

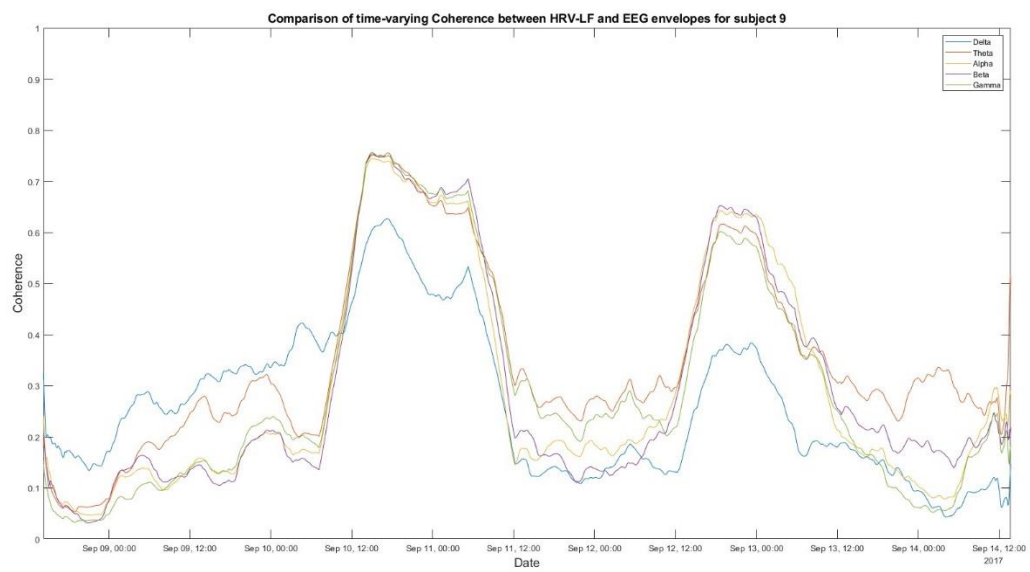
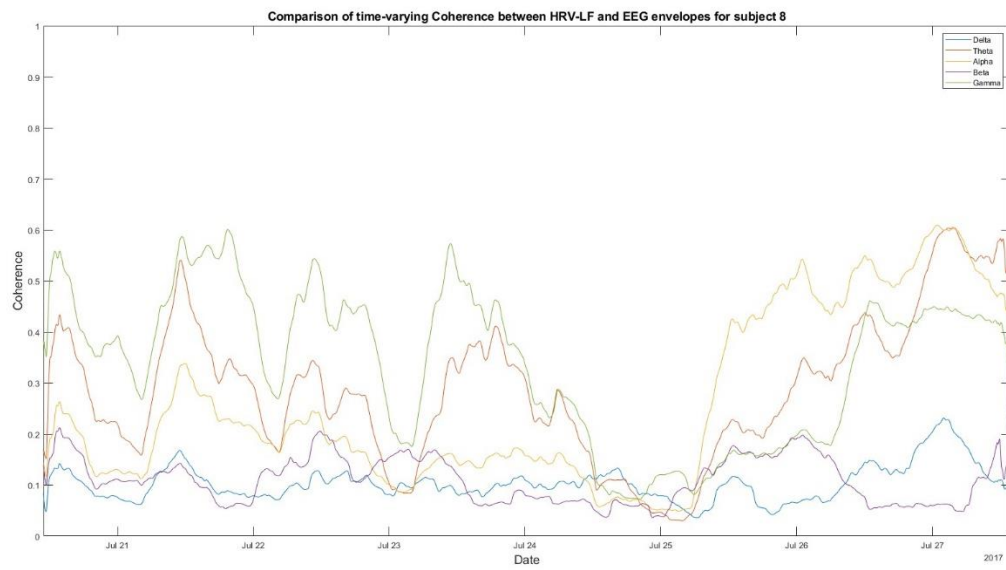
Appendix:

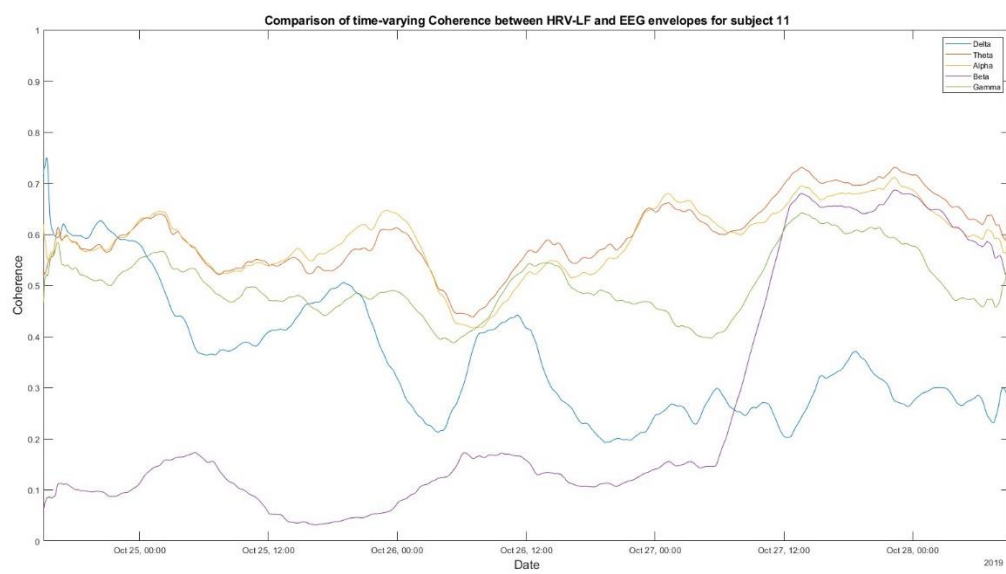
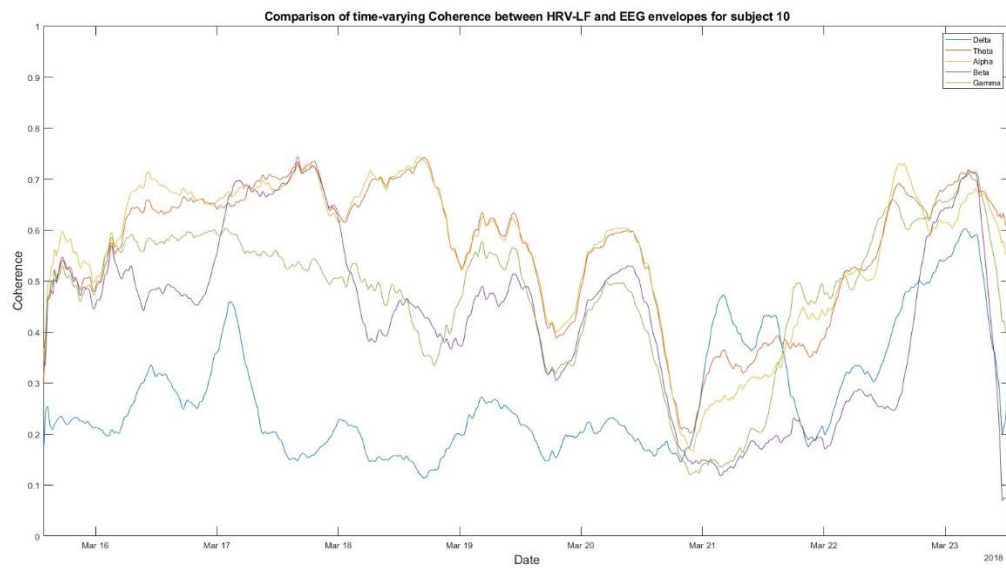
Appendix A: Brain-heart interactions for all subjects

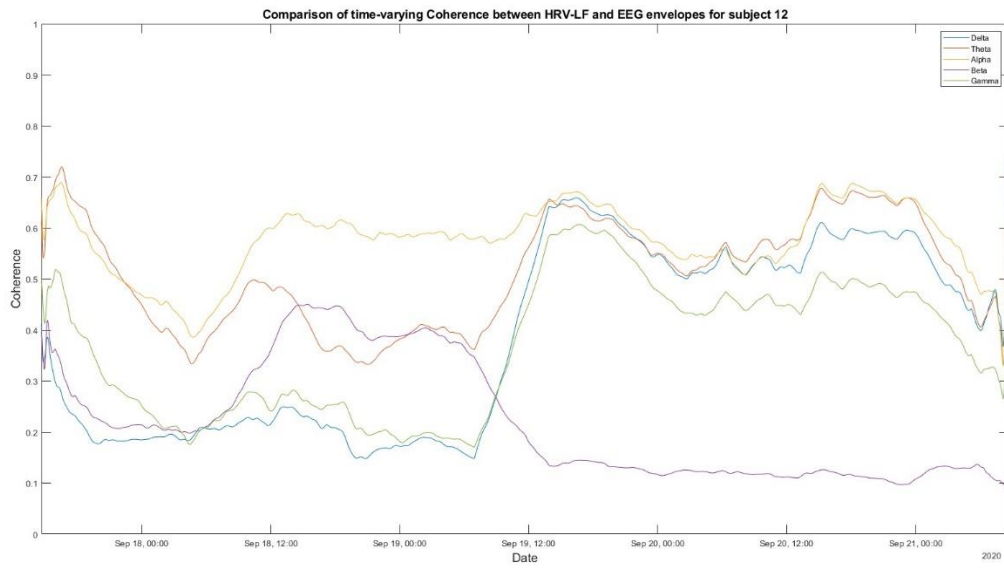




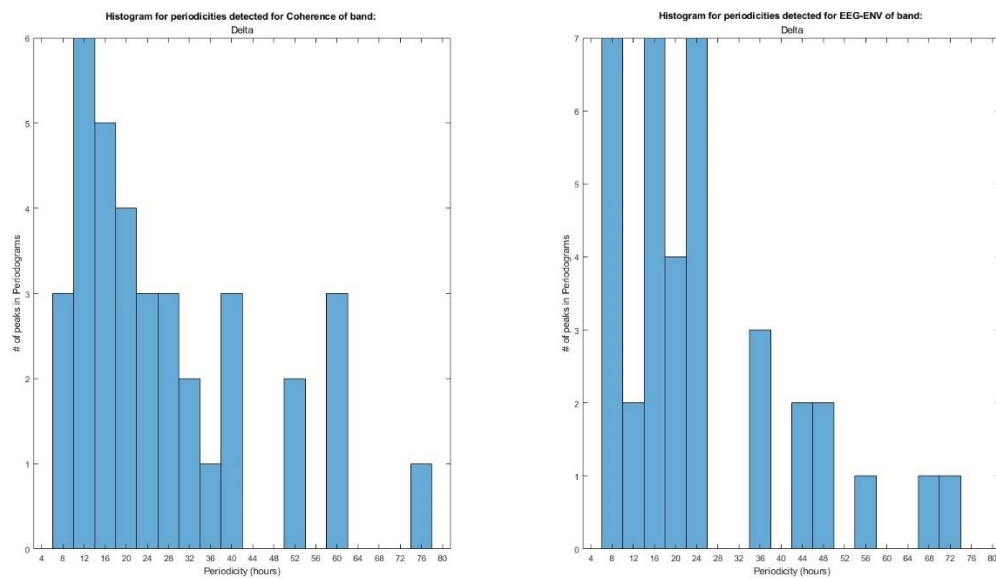


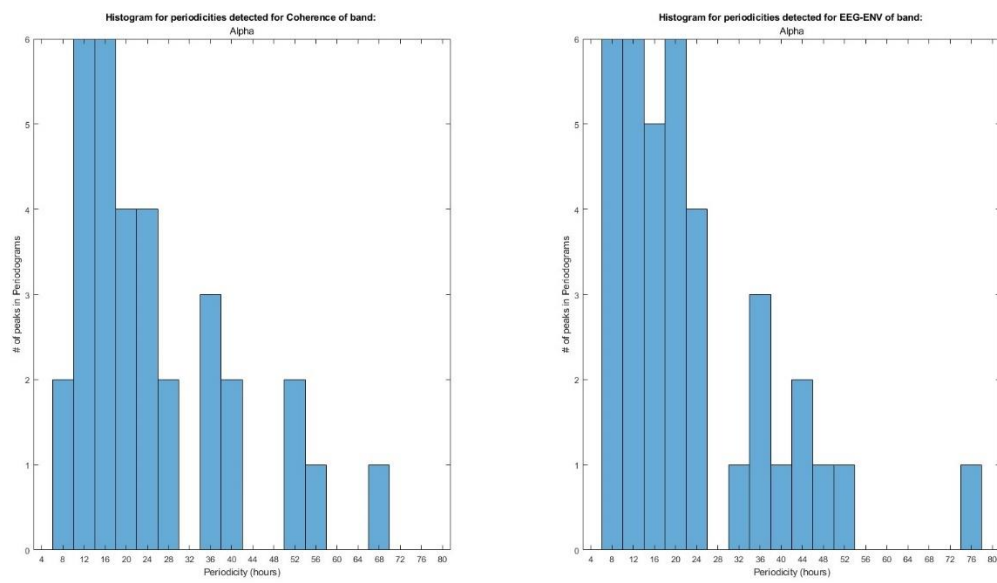
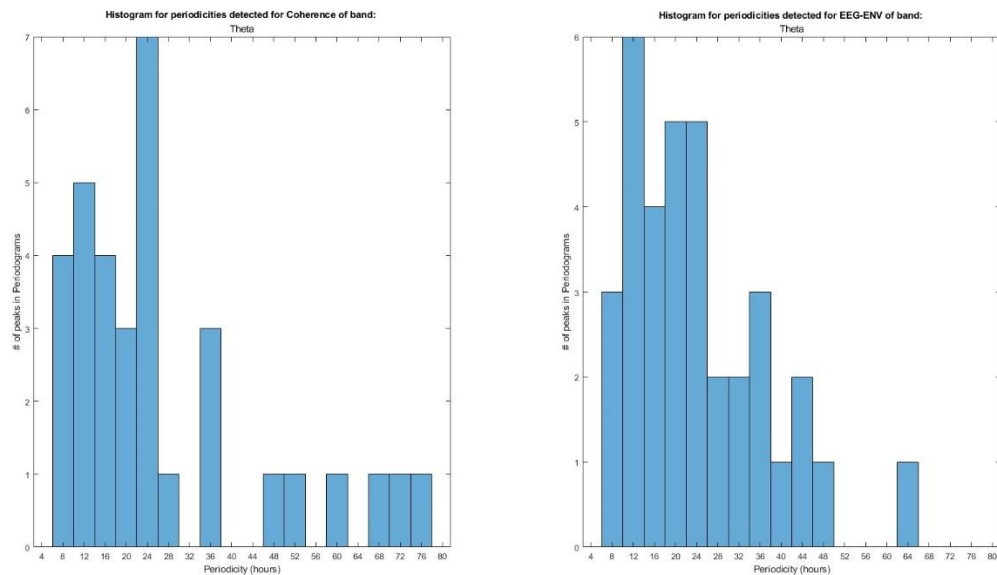


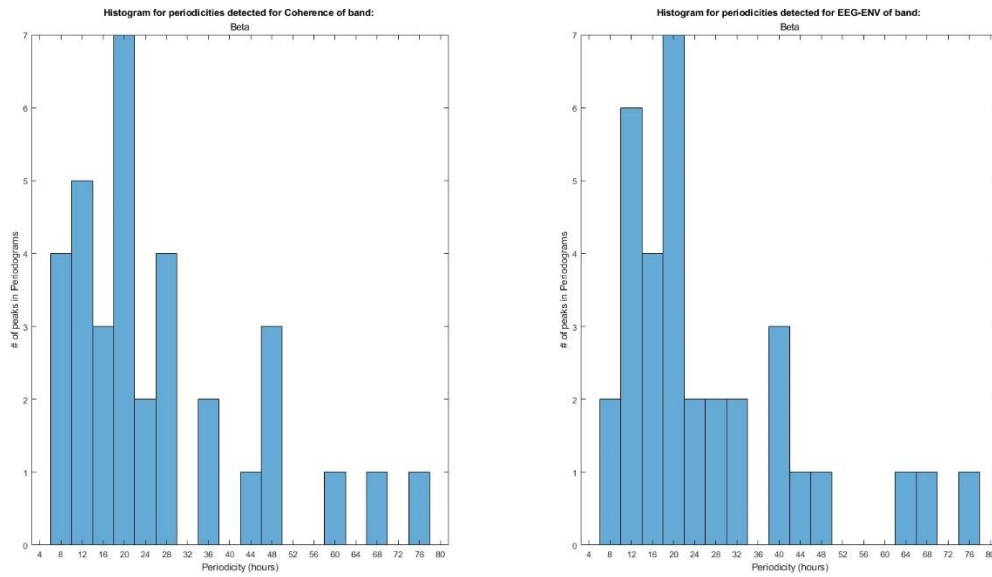




Appendix B: Histograms of detected periodicities for each signal







Appendix C: Average Periodograms for each signal

